Coordination Control of Quadrotor VTOL Aircraft in Three-Dimensional Space

K.D. Do

Abstract

This paper presents a constructive design of distributed coordination controllers for a group of N quadrotor vertical take-off and landing (VTOL) aircraft in three-dimensional space. A combination of Euler angles and unit-quaternion for the attitude representation of the aircraft is used to result in an effective control design, and to reduce singularities in the aircraft's dynamics. The coordination control design is based on a new bounded control design technique for second-order systems and new pairwise collision avoidance functions. The pairwise collision functions are functions of both relative positions and relative velocities between the aircraft instead of only their relative positions as in the literature. To overcome the inherent underactuation of the aircraft, the roll and pitch angles of the aircraft are considered as immediate controls. Simulations illustrate the results.

Index Terms

Coordination control, quadrotor aircraft, collision avoidance.

I. Introduction

Quadrotor aircraft are attractive VTOL aerial vehicles for various military and civilian applications. A quadrotor aircraft usually has a rigid cross frame equipped with two pairs of rotors, which rotate in opposite direction to compensate the reactive torques. The vertical (altitude) motion is resulted by collectively increasing and decreasing the speed of all four rotors. The pitch and roll motions are achieved by changing the speed of the front-rear pair and the left-right pair of rotors, respectively. The yaw motion is realized by the difference in reactive torques between the two pairs of the rotors. The horizontal (latitude and longitude) motions are resulted from the coupling of the roll, pitch and vertical motions. There is no change in the direction of rotation of the rotors. The motions of the quadrotor aircraft are nonlinearly coupled. Moreover, the aircraft are underactuated since there are only four independent control inputs (four rotors) while there are six degrees of freedom (latitude, longitude, altitude, roll, pitch, and yaw) to be controlled, see [1] for more details on controlling other underactuated mechanical systems. The underactuation and nonlinear coupling features of the quadrotor aircraft result in difficulties in controlling their motions. A brief review of the works on controlling single and multiple quadrotor aircraft is given below to motivate contributions of the present paper.

Due to the aforementioned difficulties, controlling a VTOL aircraft was initially restricted in a vertical plane. An input-output linearization approach was used in [2], [3], [4] to develop controllers for stabilization and output tracking/regulation of a VTOL aircraft. By noting that the output at a fixed point with respect to the aircraft body (the Huygens center of oscillation) can be used, several controllers were designed in [5], [6], [7], [8]. Since the aircraft usually operate in three-dimensional (3D) space, control of their six degrees of freedom has recently been addressed in [9], [10], [11] on local position control, [12], [13] on attitude control, and [14], [15] on global position control. In comparison with the two-dimensional (2D) case, control of the aircraft in 3D space has two main additional challenges. First, the 3D case has four independent control inputs and six outputs to be controlled. Second, there are singularities in the kinematic equations describing the motions of the aircraft if the Euler angles are used to represent its attitude. In addition to the above works, control of quadrotor aircraft under bounded control inputs has also been considered by serveral authors such as those in [16], [17], [18], [19] based on the use of nested saturation control design method [20] and its alternatives.

A number of approaches has been proposed to design coordination control systems for networked agents. Here, three common approaches are briefly mentioned. The leader-follower approach (e.g., [21], [22], [23], [24]) uses several agents as leaders and others as followers. This approach is easy to understand and ensures coordination maintenance if the leaders are disturbed but the desired coordination shape cannot be maintained if the followers are perturbed unless a feedback is implemented [25]. The behavioral approach (e.g., [26], [27]), where each agent locally reacts to actions of its neighbors, is suitable for decentralized control but is difficult in control design and stability analysis since the group's behavior cannot explicitly be defined. The virtual structure approach (e.g., [28], [29], [30], [31], [32]) treats all

Department of Mechanical Engineering, Curtin University, Perth, WA 6845, Australia
Email: duc@curtin.edu.au

the agents as a single entity, and is amenable to mathematical analysis but has difficulties in controlling critical points. The coordination control design in this paper belongs to the virtual structure approach. Although most of the existing works focus on the networked agents with first-order dynamics, cooperative control of multiple agents with second-order dynamics was also addressed (e.g. [33], [34], [35], [36]). However, the problem of bounded control has been only solved recently in [37] for the case where collision avoidance between the agents must be considered. It will be seen later that since the quadrotor aircraft are underactuated it is necessary to address the bounded control problem for the agents with second-order dynamics in order to design a coordination control system for a group of quadrotor aircraft. It is noted that the proposed control design in [37] for double integrator agents is not directly applied to the problem of coordination control for quadrotor aircraft considered in this paper because the quarotor aircraft dynamics can not be globally transformed to a double integrator. Due to the mentioned difficulties and the unsolved issue, only few results on cooperative control of multiple aircraft are available.

In most existing works (e.g, [38], [39] [40], [41]) on formation control of quadrotor aircraft, the leader-follower approach, where the leader is either a actual or a virtual aircraft or a pay-load, has been utilized since as mentioned above this approach is easy to understand and maintain the desired formation. The control design is usually based on the sliding mode, Lyapunov direct and backstepping methods. In [42] and [43], several formation controllers were designed to force a group of the quadrotor aircraft to track a desired reference linear velocity and to maintain a desired formation. In the above works, collision avoidance between the aircraft is not considered. Based on potential functions, a formation control algorithm with collision avoidance for quadrotors under bounded control forces was proposed in [44] but the results are based on linearization of the aircraft dynamics (except for the yaw dynamics) around the zero value of the roll and pitch angles.

From the above discussion, this paper proposes a design of a coordination controller for a group of the quadrotor aircraft with collision avoidance between them. First, motivated by the author's recent work [45] on controlling an underactuated omni-directional intelligent navigator in 3D space a combination of Euler angles and unit-quaternion is used for the attitude representation of the aircraft for an effective control design, and for reduce of singularities in the attitude dynamics of the aircraft when only Euler angles are used for the attitude representation. Next, a new bounded control design technique for second-order systems and new pairwise collision avoidance functions are proposed to design a distributed coordination controller. In the control design, the roll and pitch angles of the aircraft are considered as immediate controls. Therefore, the main contribution of the proposed coordination control system in this paper is the design of distributed coordination control laws for a group of quadrotor aircraft that force each aircraft almost globally asymptotically and locally exponentially tracks its reference trajectory, and guarantee no collision between aircraft under bounded control inputs. The term "almost global" is referred to the fact that the aircraft need to be initialized at non-collision conditions, see (6) in Assumption 2.1. Comparison with the aforementioned works on (coordination) control of quadrotor aircraft is detailed below to show the above advantages of the proposed coordination control design in this paper.

The bounded control designs for single aircraft in [16], [17], [18], [19] are based on the use of "linear" nested saturation control design method [20] and its alternatives. As pointed out in [20], this sort of nested saturation can only be applied to "restricted tracking" problems. Consequently, the above bounded control designs for aircraft are not applicable to design almost global coordination controllers for aircraft with collision avoidance (based on potential functions). This is because the repulsive forces approach extremely large values when a collision between aircraft tends to occur. Thus, a "nonlinear" nested saturation control design is proposed in this paper to handle the above problem, which results in an almost global bounded coordination controller with collision avoidance for aircraft, see Section III-B.

The coordination controllers proposed in [38], [39] [40], [41], [42], [43] did not address collision avoidance between aircraft. Although a coordination control design with bounded control inputs was proposed in [44], there are several drawbacks of this work. First, an on-line optimal algorithm is required to select the goal positions for avoidance of local minima because the collision avoidance design is based on the potential functions in [46]. Second, the roll and pitch angles had to be assumed to be very small so that the dynamics of the aircraft (except for the yaw dynamics) can be considered as a linear system for a design of bounded control forces based on the nested design proposed in [20], [17]. Third, no stability analysis of critical points was carried out. Basically, the closed-loop system has multiple equilibrium (critical) points due to collision avoidance taken into account but in [44] only stability of desired equilibrium points was analyzed.

The rest of the paper is organized as follows. Section II defines the control objective. Section III gives essential preliminary results. Proofs of preliminary results are given in [47], [29], [37] and Appendix A. The preliminary results are to be used in the control design in Section IV and stability analysis in Appendix B. Simulations are given in Section V. Section VI concludes the paper.

II. PROBLEM STATEMENT

A. Aircraft dynamics

Under the assumption that the aerodynamics are neglected, the Lagrangian approach results in the following equations of motion of the quadrotor aircraft i, for all $i \in \mathbb{N}$ with $\mathbb{N}$ the set of all the aircraft:

$$\begin{cases} \dot{\boldsymbol{\eta}}_{1i} = \boldsymbol{v}_{1i}, \\ \dot{\boldsymbol{v}}_{1i} = -g\boldsymbol{e}_3 + \frac{1}{m_i} f_i \boldsymbol{R}_1(\boldsymbol{q}_i)\boldsymbol{e}_3, \end{cases} \quad \begin{cases} \dot{\boldsymbol{q}}_i = \boldsymbol{R}_2(\boldsymbol{q}_i)\boldsymbol{\omega}_i, \\ \dot{\boldsymbol{\omega}}_i = -\boldsymbol{J}_i^{-1}\boldsymbol{S}(\boldsymbol{\omega}_i)\boldsymbol{J}_i\boldsymbol{\omega}_i + \boldsymbol{J}_i^{-1}\boldsymbol{\tau}_i, \end{cases} \tag{1}$$

where $\boldsymbol{e}_3 = [0\ 0\ 1]^T$, g is the gravitational acceleration, m_i is the mass of the aircraft i, $\boldsymbol{J}_i$ is the inertia matrix of the aircraft i. The vector $\boldsymbol{\eta}_{1i} = [x_i\ y_i\ z_i]^T$ denotes the (latitude, longitude, altitude) displacements of the center of mass of the aircraft i coordinated in the earth-fixed frame. The vector $\boldsymbol{v}_{1i}$ denotes the linear velocity vector of the aircraft coordinated in the earth-fixed frame. The skew-symmetric matrix $\boldsymbol{S}(\boldsymbol{x})$ is defined as $\boldsymbol{S}(\boldsymbol{x})\boldsymbol{y} = \boldsymbol{x} \times \boldsymbol{y}$ for all $\boldsymbol{x} \in \mathbb{R}^3$ and $\boldsymbol{y} \in \mathbb{R}^3$, where $'\times'$ denotes the vector cross product. The unit-quaternion $\boldsymbol{q}_i = [q_{i0}\ \bar{\boldsymbol{q}}_i^T]^T$ is a four-element vector composed of a scalar component q_{0i} and a vector component $\bar{\boldsymbol{q}}_i \in \mathbb{R}^3$ that satisfy $q_{0i}^2 + \|\bar{\boldsymbol{q}}_i\|^2 = 1$. The vector $\boldsymbol{\omega}_i$ denotes the angular velocity vector of the aircraft i coordinated in the body-fixed frame. The rotational matrix $\boldsymbol{R}_1(\boldsymbol{q}_i)$, and the matrix $\boldsymbol{R}_2(\boldsymbol{q}_i)$ are given by

$$\boldsymbol{R}_1(\boldsymbol{q}_i) = (q_{0i}^2 - \|\bar{\boldsymbol{q}}_i\|^2)\boldsymbol{I}_3 + 2\bar{\boldsymbol{q}}_i\bar{\boldsymbol{q}}_i^T + 2q_{0i}\boldsymbol{S}(\bar{\boldsymbol{q}}_i), \quad \boldsymbol{R}_2(\boldsymbol{q}_i) = \frac{1}{2}\begin{bmatrix} -\bar{\boldsymbol{q}}_i^T \\ q_{0i}\boldsymbol{I}_3 + \boldsymbol{S}(\bar{\boldsymbol{q}}_i) \end{bmatrix}, \tag{2}$$

where $\boldsymbol{I}_3$ is the 3×3 identity matrix. Note that $\boldsymbol{R}_2^T(\boldsymbol{q}_i)\boldsymbol{R}_2(\boldsymbol{q}_i) = \frac{1}{4}\boldsymbol{I}_3$. The force f_i and the moment vector $\boldsymbol{\tau}_i$ are

$$f_i = \sum_{l=1}^{4} f_{il}, \quad \boldsymbol{\tau}_i = \begin{bmatrix} (f_{i4} - f_{i2})L_i \\ (f_{i3} - f_{i1})L_i \\ (f_{i2} - f_{i1} + f_{i4} - f_{i3})E_{ia} \end{bmatrix}, \tag{3}$$

where f_{il}, $l = 1,..,4$ is the thrust generated by the l^{th} rotor along the l^{th} rotor axis of the aircraft i, L_i is the distance between the rotor and the center of mass of the aircraft i, and E_{ia} is a coefficient relating the difference in the rotor's speed to the yaw moment about the vertical body axis. The aircraft dynamics (1) is underactuated because we are interested in controlling all six outputs (latitude, longitude, altitude, roll, pitch and yaw) while there are only four independent control inputs f_{il}, $l = 1, \cdots, 4$.

For the purpose of the control design later, we let ϕ_i, θ_i, and ψ_i be the roll, pitch, and yaw angles, respectively. The unit-quaternion $\boldsymbol{q}_i$ can be written in terms of ϕ_i, θ_i, and ψ_i as follows:

$$\boldsymbol{q}_i(\boldsymbol{\eta}_{2i}) = \begin{bmatrix} \cos(\frac{\phi_i}{2})\cos(\frac{\theta_i}{2})\cos(\frac{\psi_i}{2}) + \sin(\frac{\phi_i}{2})\sin(\frac{\theta_i}{2})\sin(\frac{\psi_i}{2}) \\ \sin(\frac{\phi_i}{2})\cos(\frac{\theta_i}{2})\cos(\frac{\psi_i}{2}) - \cos(\frac{\phi_i}{2})\sin(\frac{\theta_i}{2})\sin(\frac{\psi_i}{2}) \\ \cos(\frac{\phi_i}{2})\sin(\frac{\theta_i}{2})\cos(\frac{\psi_i}{2}) + \sin(\frac{\phi_i}{2})\cos(\frac{\theta_i}{2})\sin(\frac{\psi_i}{2}) \\ \cos(\frac{\phi_i}{2})\cos(\frac{\theta_i}{2})\sin(\frac{\psi_i}{2}) - \sin(\frac{\phi_i}{2})\sin(\frac{\theta_i}{2})\cos(\frac{\psi_i}{2}) \end{bmatrix}, \tag{4}$$

with $\boldsymbol{\eta}_{2i} = [\phi_i\ \theta_i\ \psi_i]^T$. Using (4), we can write the matrix $\boldsymbol{R}_1(\boldsymbol{q}_i) = \boldsymbol{R}_1(\boldsymbol{\eta}_{2i})$ defined in (2) as

$$\boldsymbol{R}_1(\boldsymbol{\eta}_{2i}) = \begin{bmatrix} \cos(\psi_i)\cos(\theta_i) & -\sin(\psi_i)\cos(\phi_i) + \sin(\phi_i)\sin(\theta_i)\cos(\psi_i) & \sin(\psi_i)\sin(\phi_i) + \sin(\theta_i)\cos(\psi_i)\cos(\phi_i) \\ \sin(\psi_i)\cos(\theta_i) & \cos(\psi_i)\cos(\phi_i) + \sin(\phi_i)\sin(\theta_i)\sin(\psi_i) & -\cos(\psi_i)\sin(\phi_i) + \sin(\theta_i)\sin(\psi_i)\cos(\phi_i) \\ -\sin(\theta_i) & \sin(\phi_i)\cos(\theta_i) & \cos(\phi_i)\cos(\theta_i) \end{bmatrix}. \tag{5}$$

B. Coordination control objective

To design a coordination control system, it is necessary to specify a common goal for the group and initial positions and velocities of the aircraft. We therefore impose the following assumptions on the reference trajectories and initial conditions between the aircraft.

Assumption 2.1:

1) At the initial time $t_0 \geq 0$, each aircraft starts at a different location and all the aircraft do not approach each other at high relative linear velocities. Specifically, there exist strictly positive constants ε_{11} and ε_{12} such that for all $(i,j) \in \mathbb{N}$ with $i \neq j$, the following conditions hold at the initial time t_0:

$$\begin{aligned} &\|\boldsymbol{\eta}_{1ij}(t_0)\| \geq \varepsilon_{11}, \\ &\boldsymbol{\eta}_{1ij}^T(t_0)\Big(\boldsymbol{K}\boldsymbol{\eta}_{1ij}(t_0) + \boldsymbol{\Delta}_i(t_0)(\boldsymbol{v}_{1i}(t_0) - \dot{\boldsymbol{\eta}}_{1id}(t_0)) - \boldsymbol{\Delta}_j(t_0)(\boldsymbol{v}_{1j}(t_0) - \dot{\boldsymbol{\eta}}_{1jd}(t_0))\Big) \geq \varepsilon_{12}, \end{aligned} \tag{6}$$

where $\boldsymbol{K} = \text{diag}(k_1, k_2, k_3)$ with $k_1, k_2,$ and k_3 being positive constants, $\boldsymbol{\eta}_{1id}(t)$ and $\boldsymbol{\eta}_{1jd}(t)$, which will be specified below, are the reference trajectories to be tracked by the aircraft i and j, and

$$\begin{aligned}
&\boldsymbol{\eta}_{1ij}(t_0) = \boldsymbol{\eta}_{1i}(t_0) - \boldsymbol{\eta}_{1j}(t_0),\\
&\boldsymbol{\Delta}_i(t_0) = \boldsymbol{I}_3 + \frac{1}{2}(\boldsymbol{v}_{1i}(t_0) - \dot{\boldsymbol{\eta}}_{1id}(t_0)) \star (\boldsymbol{v}_{1i}(t_0) - \dot{\boldsymbol{\eta}}_{1id}(t_0)),\\
&\boldsymbol{\Delta}_j(t_0) = \boldsymbol{I}_3 + \frac{1}{2}(\boldsymbol{v}_{1j}(t_0) - \dot{\boldsymbol{\eta}}_{1jd}(t_0)) \star (\boldsymbol{v}_{1j}(t_0) - \dot{\boldsymbol{\eta}}_{1jd}(t_0)).
\end{aligned} \tag{7}$$

For a vector $\boldsymbol{x} = [x_1, x_2, ..., x_n]^T \in \mathbb{R}^n$, the operator $\star$ is defined as $\boldsymbol{x} \star \boldsymbol{x} = \text{diag}(x_1^2, x_2^2, ..., x_n^2)$.

2) The reference position vector $\boldsymbol{\eta}_{1id}(t) = [x_{id}(t)\ y_{id}(t)\ z_{id}(t)]^T$ for the aircraft i to track is differentiable up to four times and satisfies the following conditions:

$$\begin{aligned}
&\|\boldsymbol{\eta}_{1id}(t) - \boldsymbol{\eta}_{1jd}(t)\| \geq \varepsilon_2,\\
&\dot{\boldsymbol{\eta}}_{1id}(t) = \dot{\boldsymbol{\eta}}_{1jd}(t),\ \ddot{\boldsymbol{\eta}}_{1id}(t) = \ddot{\boldsymbol{\eta}}_{1jd}(t),
\end{aligned} \tag{8}$$

for all $(i, j) \in \mathbb{N}$, $j \neq i$ and $t \geq t_0$, where ε_2 is a positive constant. Moreover, the absolute value of the second derivative of $z_{id}(t)$ is assumed to be strictly less than g, i.e.,

$$\sup_{t \in \mathbb{R}^+} |\ddot{z}_{id}(t)| \leq g - \varrho, \tag{9}$$

where ϱ is a strictly positive constant. The reference yaw angle $\psi_{id}(t)$ is assumed to be twice differentiable.

Coordination Control Objective 2.1: Under Assumption 2.1, for each aircraft i design the control inputs f_{il}, $l = 1, \cdots, 4$ such that the position vector $\boldsymbol{\eta}_{1i}(t)$ and the yaw angle $\psi_i(t)$ of the aircraft i track their reference trajectories $\boldsymbol{\eta}_{1id}(t)$ and $\psi_{id}(t)$, respectively, and there is no collision with all other aircraft in the group. Specifically, we will design the control inputs f_{il}, $l = 1, \cdots, 4$ for the aircraft i such that

$$\begin{aligned}
&\lim_{t \to \infty} (\boldsymbol{\eta}_{1i}(t) - \boldsymbol{\eta}_{1id}(t)) = 0, \quad \lim_{t \to \infty} (\psi_i(t) - \psi_{id}(t)) = 0,\\
&\|\boldsymbol{\eta}_{1i}(t) - \boldsymbol{\eta}_{1j}(t)\| \geq \varepsilon_3,
\end{aligned} \tag{10}$$

for all $(i, j) \in \mathbb{N}$, $i \neq j$ and $t \geq t_0 \geq 0$, where ε_3 is a strictly positive constant. Moreover, the control design needs to keep all other states of the aircraft dynamics bounded for all initial conditions $\boldsymbol{\eta}_{1i}(t_0) \in \mathbb{R}^3$ and $\boldsymbol{v}_{1i}(t_0) \in \mathbb{R}^3$ satisfying (6), and $\boldsymbol{q}_i(t_0) \in \mathbb{R}^3$ with $\|\boldsymbol{q}_i(t_0)\|^2 = 1$, and $\boldsymbol{\omega}_i(t_0) \in \mathbb{R}^3$.

Remark 2.1:

1) If at the initial time t_0 the aircraft approached each other at high relative linear velocities, the controls f_{il}, $l = 1, \cdots, 4$ would not be able to prevent the aircraft from colliding with each other because the aircraft are underactuated, see Section IV for more details. Therefore, it is reasonable to impose Assumption 2.1.1 for the design of the controls f_{il} for all $i = 1, ..., N$ and $l = 1, \cdots, 4$, which guarantee collision avoidance between the aircraft.
2) Assumption 2.1.2 specifies feasible reference trajectories $\boldsymbol{\eta}_{1id}(t)$ with $i \in \mathbb{N}$ for the aircraft to track since they have to satisfy the conditions listed in (8). A desired coordination shape can be specified by the reference trajectories $\boldsymbol{\eta}_{1id}(t)$ with $i \in \mathbb{N}$. Let us consider the virtual structure approach in [48], [29] to generate the reference trajectories $\boldsymbol{\eta}_{1id}(t)$ with $i \in \mathbb{N}$. First, a virtual structure consisting of N vertices is designed as a desired coordination shape. Second, we let the center of the virtual structure move along the common reference trajectory $\boldsymbol{\eta}_{1od}(t)$. Third, as the virtual structure moves, its vertex i generates the reference trajectory $\boldsymbol{\eta}_{1id}(t)$. Specifically, the reference trajectory $\boldsymbol{\eta}_{1id}(t)$ can be generated as $\boldsymbol{\eta}_{1id}(t) = \boldsymbol{\eta}_{1od}(t) + \boldsymbol{l}_i$ where $\boldsymbol{l}_i$ is a constant vector. The second equation of (8) implies that all the aircraft have the same desired linear velocity and acceleration. As such, this approach also applies to the case where uniform expansion or contraction of the desired virtual structure in the sense that the vectors $\boldsymbol{l}_i$ are time-varying but need to satisfy the conditions

$$\begin{aligned}
&\dot{\boldsymbol{l}}_i = \dot{\boldsymbol{l}}_j,\ \ddot{\boldsymbol{l}}_i = \ddot{\boldsymbol{l}}_j,\\
&\|\boldsymbol{l}_i(t) - \boldsymbol{l}_j(t)\| \geq \varepsilon_2,\ \forall\, t \geq t_0 \geq 0,
\end{aligned} \tag{11}$$

for all $(i, j) \in \mathbb{N}$, $j \neq i$, where ε_2 is the positive constant as defined in (8), and $\|\dot{\boldsymbol{l}}_i\|$ and $\|\ddot{\boldsymbol{l}}_i\|$ are bounded. Basically, the above conditions imply that all the aircraft have the same desired linear velocity and acceleration, i.e., $\dot{\boldsymbol{\eta}}_{1id}(t) = \dot{\boldsymbol{\eta}}_{1jd}(t)$, and $\ddot{\boldsymbol{\eta}}_{1id}(t) = \ddot{\boldsymbol{\eta}}_{1jd}(t)$. This requirement is to make it possible to affine the control f_i in the derivative of proper Lyapunov function for the control design, see the paragraph just after (35).
3) The conditions listed (8) in Assumption 2.1.2 also implies that the approach in this paper excludes cases like Rendez-

vous or flocking where no reference position is assigned to the group, or to a virtual center of the formation, and a specified formation shape is required.

4) The condition (9) implies that the aircraft are not allowed to land faster than it freely falls under the gravitational force. We specify this condition to design smooth controls f_{il} for all $i = 1, ..., N$ and $l = 1, \cdots, 4$ to obtain "almost global coordination" tracking results. The term "almost global coordination" is referred to the fact that the initial conditions (6) hold.
5) There is a common point between this paper and the aforementioned works ([38], [39] [40], [41]) on formation control of aircraft in the sense that each aircraft has its own reference trajectory to track. The main difference is the collision avoidance objective, i.e., the condition 3 in (10). Although this condition was not explicitly stated in [44], the formation control design in [44] did consider this condition. However, there are drawbacks in [44] as mentioned in the previous section.

III. Preliminaries

This section presents saturation functions, a technique for designing bounded controllers for a second-order system, a non-zero convergent lemma for a differential inequality, smooth step functions, and Barbalat-like lemma. These preliminary results will be used in the control design and stability analysis later.

A. Saturation functions

Definition 3.1: The function $\sigma(x)$ is said to be a smooth saturation function if it possesses the following properties:

$$\begin{aligned}&\sigma(x) = 0 \text{ if } x = 0,\ \sigma(x)x > 0 \text{ if } x \neq 0,\\&\sigma(-x) = -\sigma(x),\ (x-y)[\sigma(x)-\sigma(y)] \geq 0,\\&|\sigma(x)| \leq 1,\ |\frac{\sigma(x)}{x}| \leq 1,\ |\frac{\partial \sigma(x)}{\partial x}| \leq 1,\end{aligned}$$

for all $(x, y) \in \mathbb{R}^2$.
Some functions satisfying the above properties include $\sigma(x) = \tanh(x)$ and $\sigma(x) = \frac{x}{\sqrt{1+x^2}}$. For the vector $\boldsymbol{x} = [x_1, \cdots, x_n]^T$, we use the notation $\boldsymbol{\sigma}(\boldsymbol{x}) = [\sigma(x_1), \cdots, \sigma(x_n)]^T$ to denote the smooth saturation function vector of $\boldsymbol{x}$.

B. Bounded control design for second-order systems

Lemma 3.1: Consider the following second-order system:

$$\begin{aligned}\dot{x}_1 &= x_2,\\ \dot{x}_2 &= u,\end{aligned} \tag{12}$$

where x_1 and x_2 are the states, and u is the control input. Let the positive constants k and c be chosen such that $0.5k + c \leq u^{\max}$ with $u^{\max}$ being a strictly positive constant, and let $\sigma(\bullet)$ be a smooth saturation function of $\bullet$ defined in Definition 3.1. The bounded control law

$$u = \frac{1}{1+1.5x_2^2}\Big(-kx_2 - c\sigma\Big(kx_1 + \big(1+0.5x_2^2\big)x_2\Big)\Big) \tag{13}$$

globally asymptotically stabilizes the system (12) at the origin and satisfies $|u(t)| \leq u^{\max}$ for all $t \geq t_0 \geq 0$ and initial values $(x_1(t_0), x_2(t_0)) \in \mathbb{R}^2$.
Proof. See [37]. The main difference between the bounded control law (13) and those, which are appeared in [16], [17], [18], [19], [44], based on the nested saturation control design (e.g., [20], [49]) is the term $1+1.5x_2^2$. This important term motivates the design of a bounded formation controller with collision avoidance between aircraft in the next section.

C. Non-zero convergent lemma

This subsection presents a non-zero convergent result for a first-order system. This result will be used to construct pairwise collision avoidance functions in Subsection IV-A2.

Lemma 3.2: Assume that the vectors $\boldsymbol{x}_1 \in \mathbb{R}^n$ and $\boldsymbol{x}_2 \in \mathbb{R}^n$ satisfy the following conditions

$$\begin{aligned}&\|\boldsymbol{x}_{12}(t_0)\| \geq a_0,\\&\boldsymbol{x}_{12}^T\Big[\Big(\boldsymbol{I}_n + \frac{1}{2}(\dot{\boldsymbol{x}}_1 - \boldsymbol{\mu}(t)) \star (\dot{\boldsymbol{x}}_1 - \boldsymbol{\mu}(t))\Big)(\dot{\boldsymbol{x}}_1 - \boldsymbol{\mu}(t)) - \Big(\boldsymbol{I}_n + \frac{1}{2}(\dot{\boldsymbol{x}}_2 - \boldsymbol{\mu}(t)) \star (\dot{\boldsymbol{x}}_2 - \boldsymbol{\mu}(t))\Big)(\dot{\boldsymbol{x}}_2 - \boldsymbol{\mu}(t)) + \boldsymbol{B}\boldsymbol{x}_{12}\Big] \geq a,\end{aligned} \tag{14}$$

for all $t \geq t_0 \geq 0$, where $\boldsymbol{x}_{12} = \boldsymbol{x}_1 - \boldsymbol{x}_2$, $t_0 \geq 0$ is the initial time, $\boldsymbol{I}_n$ is the $n \times n$ identity matrix, $\boldsymbol{\mu}(t) \in \mathbb{R}^n$ is a vector whose elements are bounded functions of t, $\boldsymbol{B}$ is a symmetric positive definite matrix, a_0 and a are strictly positive constants. Then

$$\|\boldsymbol{x}_{12}(t)\| \geq \min\left(a_0, \sqrt{\frac{a}{\lambda_M(\boldsymbol{B})}}\right) \tag{15}$$

for all $t \geq t_0 \geq 0$, where $\lambda_M(\boldsymbol{B})$ is the maximum eigenvalue of the matrix $\boldsymbol{B}$.

Proof. See Appendix A.

D. Smooth step function

This subsection gives a definition of the smooth step function followed by a construction of this function. The smooth step function is to be embedded in a pairwise collision avoidance function to avoid discontinuities in the control law in solving the collision avoidance problem.

Definition 3.2: A scalar function $h(x, a, b)$ is said to be a smooth step function if it is smooth and possesses the following properties:

$$\begin{array}{ll} 1)\ h(x,a,b) = 0,\ \forall x \in (-\infty, a], & 3)\ 0 < h(x,a,b) < 1,\ \forall x \in (a,b), \\ 2)\ h(x,a,b) = 1,\ \forall x \in [b, \infty), & 4)\ h'(x,a,b) > 0,\ \forall x \in (a,b), \end{array} \tag{16}$$

where $h'(x,a,b) = \frac{\partial h(x,a,b)}{\partial x}$, and a and b are constants such that $a < b$.

Lemma 3.3: Let the scalar function $h(x, a, b)$ be defined as

$$h(x,a,b) = \frac{f(\tau)}{f(\tau) + f(1-\tau)} \text{ with } \tau = \frac{x-a}{b-a}, \tag{17}$$

where $f(\tau) = 0$ if $\tau \leq 0$ and $f(\tau) = e^{-\frac{1}{\tau}}$ if $\tau > 0$, with a and b being constants such that $a < b$. Then the function $h(x, a, b)$ is a smooth step function.

Proof. See [47].

E. Barbalat-like lemma

The following Barbalat-like lemma is to be used in the stability analysis of the closed-loop system.

Lemma 3.4: Assume that a nonnegative scalar differentiable function $f(t)$ satisfies the following conditions

$$1) \left|\frac{d}{dt} f(t)\right| \leq k_1 f(t), \forall t \geq 0,\ \ 2) \int_0^\infty f(t) dt \leq k_2 \tag{18}$$

where k_1 and k_2 are positive constants, then $\lim_{t \to \infty} f(t) = 0$.

Proof. See [29]. Lemma 3.4 differs from Barbalat's lemma found in [50]. While Barbalat's lemma assumes that $f(t)$ is uniformly continuous, Lemma 3.4 assumes that $|\frac{d}{dt} f(t)|$ is bounded by $k_1 f(t)$. Lemma 3.4 is useful in proving convergence of $f(t)$ when it is difficult to prove uniform continuity of $f(t)$.

IV. Control Design

The control design consists of two stages. In the first stage, the first two equations of (1) will be considered. Using the bounded control design for second-order systems in Subsection III-B and the pairwise collision avoidance functions in Subsection IV-A2, we will design the total thrust f_i and the virtual controls of the roll angle ϕ_i and the pitch angle θ_i of the aircraft i. These controls are designed such that there is no collision between any aircraft and the tracking error $\boldsymbol{\eta}_{1i}(t) - \boldsymbol{\eta}_{1id}(t)$ is asymptotically stabilized at the origin. In the second stage, the last two equations of (1) will be considered. Using the backstepping technique [51] the moment vector $\boldsymbol{\tau}_i$ will be designed to globally asymptotically and locally exponentially stabilize the tracking error $\psi_i(t) - \psi_{id}(t)$ and the errors between the virtual controls of the roll and pitch angles and their actual values at the origin.

A. Stage 1

1) Tracking and virtual control errors: We define

$$\begin{aligned} \boldsymbol{\eta}_{1ie} &= \boldsymbol{\eta}_{1i} - \boldsymbol{\eta}_{1id}, \\ \boldsymbol{v}_{1ie} &= \boldsymbol{v}_{1i} - \dot{\boldsymbol{\eta}}_{1id}, \\ \boldsymbol{q}_{ie} &= \boldsymbol{q}_i - \boldsymbol{\alpha}_{\boldsymbol{q}_i} \end{aligned} \tag{19}$$

where $\boldsymbol{\alpha}_{\boldsymbol{q}_i} = [\alpha_{q_{0i}}\ \boldsymbol{\alpha}_{\bar{\boldsymbol{q}}_i}^T]^T$ with $\boldsymbol{\alpha}_{\bar{\boldsymbol{q}}_i} = [\alpha_{q_{1i}}\ \alpha_{q_{2i}}\ \alpha_{q_{3i}}]^T$ is a virtual control of $\boldsymbol{q}_i$. It is noted that either $-\alpha_{\boldsymbol{q}_i}$ or $+\alpha_{\boldsymbol{q}_i}$ can be used in the third equation of (19) and results in the same desired orientation of the aircraft when $\boldsymbol{q}_{ie}$ is equal to zero. This is because from (4) we have $\boldsymbol{q}_i(\boldsymbol{\eta}_{2i}) = -\boldsymbol{q}_i(\boldsymbol{\eta}_{2i} - 2\pi)$. Therefore, $-\boldsymbol{\alpha}_{\boldsymbol{q}_i}$ represents the desired Euler angles corresponding to those, which are represented by $+\boldsymbol{\alpha}_{\boldsymbol{q}_i}$, are rotated by an angle of 2π. Substituting the third equation of (19) into (2) results in

$$\boldsymbol{R}_1(\boldsymbol{q}_i) = \boldsymbol{R}_1(\boldsymbol{\alpha}_{\boldsymbol{q}_i}) + \boldsymbol{H}(\boldsymbol{q}_{ie}, \boldsymbol{\alpha}_{\boldsymbol{q}_i}), \tag{20}$$

where

$$\boldsymbol{H}(\boldsymbol{q}_{ie}, \boldsymbol{\alpha}_{\boldsymbol{q}_i}) = \Big[q_{0ie}(q_{0ie} - 2\alpha_{q_{0i}}) - \bar{\boldsymbol{q}}_{ie}^T(\bar{\boldsymbol{q}}_{ie} - 2\boldsymbol{\alpha}_{\bar{\boldsymbol{q}}_i})\Big]\boldsymbol{I}_3 + 2\bar{\boldsymbol{q}}_{ie}(\bar{\boldsymbol{q}}_{ie}^T - 2\boldsymbol{\alpha}_{\bar{\boldsymbol{q}}_i}^T) + 2\Big[q_{0ie}(\boldsymbol{S}(\bar{\boldsymbol{q}}_{ie}) - \boldsymbol{S}(\boldsymbol{\alpha}_{\bar{\boldsymbol{q}}_i})) - \alpha_{q_{0i}}\boldsymbol{S}(\bar{\boldsymbol{q}}_{ie})\Big], \tag{21}$$

since $\boldsymbol{S}(\boldsymbol{x} + \boldsymbol{y}) = \boldsymbol{S}(\boldsymbol{x}) + \boldsymbol{S}(\boldsymbol{y})$ for all $\boldsymbol{x} \in \mathbb{R}^3$ and $\boldsymbol{y} \in \mathbb{R}^3$. Now let us define $\boldsymbol{\alpha}_{\boldsymbol{\eta}_{2i}} = [\alpha_{\phi_i}\ \alpha_{\theta_i}\ \alpha_{\psi_i}]^T$ with

$$\alpha_{\psi_i} = \psi_{id}, \tag{22}$$

which is the virtual control of $\boldsymbol{\eta}_{2i}$ corresponding to the virtual unit-quaternion vector $\boldsymbol{\alpha}_{\boldsymbol{q}_i}$. Using (5), we can write $\boldsymbol{R}_1(\boldsymbol{\alpha}_{\boldsymbol{q}_i}) = \boldsymbol{R}_1(\boldsymbol{\alpha}_{\boldsymbol{\eta}_{2i}})$ as

$$\boldsymbol{R}_1(\boldsymbol{\alpha}_{\boldsymbol{q}_i}) = \boldsymbol{R}_1(\boldsymbol{\eta}_{2i})\big|_{\boldsymbol{\eta}_{2i} = \boldsymbol{\alpha}_{\boldsymbol{\eta}_{2i}}}, \tag{23}$$

where using (4) we have the relationship between $\boldsymbol{\alpha}_{\boldsymbol{q}_i}$ and $\boldsymbol{\alpha}_{\boldsymbol{\eta}_{2i}}$ as follows:

$$\boldsymbol{\alpha}_{\boldsymbol{q}_i} = \boldsymbol{q}_i(\boldsymbol{\eta}_{2i})\big|_{\boldsymbol{\eta}_{2i} = \boldsymbol{\alpha}_{\boldsymbol{\eta}_{2i}}}. \tag{24}$$

The purpose of writing down (23) and (24) is that it is difficult to directly design the virtual control $\boldsymbol{\alpha}_{\boldsymbol{q}_i}$. Therefore, we will design the virtual control $\boldsymbol{\alpha}_{\boldsymbol{\eta}_{2i}}$ (only α_{ϕ_i} and α_{θ_i} since α_{ψ_i} is already available in (22)) by using (23) then the virtual control $\boldsymbol{\alpha}_{\boldsymbol{q}_i}$ will be found by substituting $\boldsymbol{\alpha}_{\boldsymbol{\eta}_{2i}}$ into (24). With the second equation of (19), (20), and the first equation of (1), we can write $\dot{\boldsymbol{v}}_{1ie}$ as

$$\dot{\boldsymbol{v}}_{1ie} = -g\boldsymbol{e}_3 + \frac{f_i}{m_i}\boldsymbol{R}_1(\boldsymbol{\alpha}_{\boldsymbol{q}_i})\boldsymbol{e}_3 - \ddot{\boldsymbol{\eta}}_{1id} + \frac{f_i}{m_i}\boldsymbol{H}(\boldsymbol{q}_{ie}, \boldsymbol{\alpha}_{\boldsymbol{q}_i})\boldsymbol{e}_3. \tag{25}$$

2) Pairwise collision avoidance functions: This subsection defines and constructs pairwise collision avoidance functions. In constructing these functions, we utilize Lemma 3.2, Definition 3.2, and Lemma 3.3. The pairwise collision avoidance functions will be used for the coordination control design in the next section.

Definition 4.1: Let β_{ij} with $(i,j) \in \mathbb{N}$ and $i \neq j$ be a scalar function of χ_{ij}, which is given by

$$\chi_{ij} = \boldsymbol{\eta}_{1ij}^T\Big(\boldsymbol{K}\boldsymbol{\eta}_{1ij} + \boldsymbol{\Delta}_i\boldsymbol{v}_{1ie} - \boldsymbol{\Delta}_j\boldsymbol{v}_{1je}\Big), \tag{26}$$

where is the diagonal positive definite matrix defined in (6) and

$$\begin{aligned}
&\boldsymbol{\eta}_{1ij} = \boldsymbol{\eta}_{1i} - \boldsymbol{\eta}_{1j},\\
&\boldsymbol{\Delta}_i = \boldsymbol{I}_3 + \frac{1}{2}\boldsymbol{v}_{1ie} \star \boldsymbol{v}_{1ie},\ \boldsymbol{\Delta}_j = \boldsymbol{I}_3 + \frac{1}{2}\boldsymbol{v}_{1je} \star \boldsymbol{v}_{1je}.
\end{aligned} \tag{27}$$

The function β_{ij} is said to be a pairwise collision avoidance function if it possesses the following properties:

$$\begin{aligned}
&1)\ \beta_{ij} = 0,\ \beta'_{ij} = 0,\ \beta''_{ij} = 0,\ \beta'''_{ij} = 0,\ \forall\, \chi_{ij} \in [\chi^*_{ij}, \infty),\\
&2)\ \beta_{ij} > 0,\ \forall\, \chi_{ij} \in (0, \chi^*_{ij}),\ \beta'_{ij} \leq 0,\ \forall\, \chi_{ij} \in \mathbb{R},\\
&3)\ \lim_{\chi_{ij}\to 0} \beta_{ij} = \infty,\ \lim_{\chi_{ij}\to 0} \beta'_{ij} = -\infty,\ \lim_{\chi_{ij}\to 0} \beta''_{ij} = -\infty,\\
&4)\ \beta_{ij}\ \text{ is smooth},\ \forall\, \chi_{ij} \in (0, \infty),
\end{aligned} \tag{28}$$

where $\beta'_{ij} = \frac{\partial \beta_{ij}}{\partial \chi_{ij}}$, $\beta''_{ij} = \frac{\partial^2 \beta_{ij}}{\partial \chi^2_{ij}}$, $\beta''_{ij} = \frac{\partial^3 \beta_{ij}}{\partial \chi^3_{ij}}$, and the constant χ^*_{ij} is strictly positive and is chosen such that

$$\chi^*_{ij} \leq \chi_{ijd}, \tag{29}$$

with $\chi_{ijd} = \chi_{ij}\big|_{\boldsymbol{\eta}_{1i} = \boldsymbol{\eta}_{1id}, \boldsymbol{\eta}_{1j} = \boldsymbol{\eta}_{1jd}, \boldsymbol{v}_{1i} = \dot{\boldsymbol{\eta}}_{1id}, \boldsymbol{v}_{1j} = \dot{\boldsymbol{\eta}}_{1jd}}$, i.e.,

$$\begin{aligned}
\chi_{ijd} &= \boldsymbol{\eta}_{1ijd}^T\boldsymbol{K}\boldsymbol{\eta}_{1ijd},\\
\boldsymbol{\eta}_{1ijd} &= \boldsymbol{\eta}_{1id} - \boldsymbol{\eta}_{1jd}.
\end{aligned} \tag{30}$$

Remark 4.1: Property 1) implies that the function β_{ij} is zero when the aircraft i and j are at their desired locations or are sufficiently faraway from each other and do not approach each other at a high relative linear velocity since the constant χ^*_{ij} satisfies the condition (29). Property 2) implies that the function β_{ij} is positive when the aircraft i and j are sufficiently close to each other and/or are approaching each other at a high relative linear velocity. Property 3) means that the function β_{ij} is equal to infinity when a collision between the agents i and j occurs. Property 4) allows us to use control design and stability analysis methods found in [50] for continuous systems instead of techniques for switched and discontinuous systems found in [52] to handle the collision avoidance problem.

Using the smooth step function given in Definition 3.2, we can find many functions that satisfy all the properties listed in (28). An example is

$$\beta_{ij} = d_{ij}\frac{1 - h(\chi_{ij}, a_{ij}, b_{ij})}{h(\chi_{ij}, a_{ij}, b_{ij})}, \tag{31}$$

where d_{ij} is a positive constant, and the positive constants a_{ij} and b_{ij} satisfy the condition

$$0 < a_{ij} < b_{ij} \leq \chi^*_{ij}. \tag{32}$$

The function $h\big(\chi_{ij}, a_{ij}, b_{ij}\big)$ is a smooth step function defined in Definition 3.2. It can be directly verified that the function β_{ij} given in (31) possesses all the properties listed in (28). The function β_{ij} defined in (31) will be used in the rest of the paper.

3) Design of f_i and $\boldsymbol{\alpha}_{\boldsymbol{\eta}_{2i}}$: To design the control f_i and the virtual control $\boldsymbol{\alpha}_{\boldsymbol{\eta}_{2i}}$, we consider the following Lyapunov-like function:

$$V_1 = \frac{1}{2}\bigg(\sum_{i=1}^{N}\|2\boldsymbol{K}\boldsymbol{\eta}_{1ie} + \boldsymbol{\Delta}_i\boldsymbol{v}_{1ie}\|^2 + \sum_{i=1}^{N}\sum_{j\in\mathbb{N}_i}\beta_{ij}\bigg), \tag{33}$$

where the matrices $\boldsymbol{K}$ and $\boldsymbol{\Delta}_i$, and the pairwise collision avoidance function β_{ij} are given in Definition 4.1, and $\mathbb{N}_i$ is the set containing all the aircraft except for the aircraft i. Differentiating both sides of (33) gives

$$\dot{V}_1 = \sum_{i=1}^{N}\boldsymbol{\Omega}_i^T\Big(2\boldsymbol{K}\boldsymbol{v}_{1ie} + (\boldsymbol{\Delta}_i + \boldsymbol{v}_{1ie}\star\boldsymbol{v}_{1ie})\dot{\boldsymbol{v}}_{1ie}\Big) + \frac{1}{2}\sum_{i=1}^{N}\sum_{j\in\mathbb{N}_i}\beta'_{ij}\boldsymbol{v}_{1ij}^T(\boldsymbol{\Delta}_i\boldsymbol{v}_{1ie} - \boldsymbol{\Delta}_j\boldsymbol{v}_{1je}), \tag{34}$$

where

$$\boldsymbol{\Omega}_i = 2\boldsymbol{K}\boldsymbol{\eta}_{1ie} + \boldsymbol{\Delta}_i\boldsymbol{v}_{1ie} + \sum_{j\in\mathbb{N}_i}\beta'_{ij}\boldsymbol{\eta}_{1ij}. \tag{35}$$

Since $\dot{\boldsymbol{\eta}}_{1id} = \dot{\boldsymbol{\eta}}_{1jd}$, see (8), we have $\boldsymbol{v}_{1ij} = \boldsymbol{v}_{1i} - \dot{\boldsymbol{\eta}}_{1id} - (\boldsymbol{v}_{1j} - \dot{\boldsymbol{\eta}}_{1jd}) = \boldsymbol{v}_{1ie} - \boldsymbol{v}_{1je}$. Hence using the equality $\boldsymbol{v}_{1ij} = \boldsymbol{v}_{1ie} - \boldsymbol{v}_{1je}$ and definition of $\boldsymbol{\Delta}_i$ and $\boldsymbol{\Delta}_j$ in (27) results in $\boldsymbol{v}_{1ij}^T(\boldsymbol{\Delta}_i\boldsymbol{v}_{1ie} - \boldsymbol{\Delta}_j\boldsymbol{v}_{1je}) \geq 0$ for all $\boldsymbol{v}_{1ie} \in \mathbb{R}^3$ and $\boldsymbol{v}_{1je} \in \mathbb{R}^3$. Now, since $\beta'_{ij} \leq 0$ for all $\chi_{ij} \in \mathbb{R}$, see Properties of β_{ij} listed in (28), we can write (34) as

$$\dot{V}_1 \leq \sum_{i=1}^{N}\boldsymbol{\Omega}_i^T\Big(2\boldsymbol{K}\boldsymbol{v}_{1ie} + (\boldsymbol{\Delta}_i + \boldsymbol{v}_{1ie}\star\boldsymbol{v}_{1ie})\dot{\boldsymbol{v}}_{1ie}\Big). \tag{36}$$

Substituting (25) into (36) yields

$$\dot{V}_1 \leq \sum_{i=1}^{N}\boldsymbol{\Omega}_i^T\Big[2\boldsymbol{K}\boldsymbol{v}_{1ie} + (\boldsymbol{\Delta}_i + \boldsymbol{v}_{1ie}\star\boldsymbol{v}_{1ie})\Big(- g\boldsymbol{e}_3 + \frac{f_i}{m_i}\boldsymbol{R}_1(\boldsymbol{\alpha}_{\boldsymbol{q}_i})\boldsymbol{e}_3 - \ddot{\boldsymbol{\eta}}_{1id}\Big)\Big] + \sum_{i=1}^{N}\boldsymbol{\Omega}_i^T\frac{f_i}{m_i}\boldsymbol{H}(\boldsymbol{q}_{ie}, \boldsymbol{\alpha}_{\boldsymbol{q}_i})\boldsymbol{e}_3. \tag{37}$$

which suggests that we choose

$$f_i\boldsymbol{R}_1(\boldsymbol{\alpha}_{\boldsymbol{q}_i})\boldsymbol{e}_3 = m_i\Big[g\boldsymbol{e}_3 + \ddot{\boldsymbol{\eta}}_{1id} + (\boldsymbol{\Delta}_i + \boldsymbol{v}_{1ie}\star\boldsymbol{v}_{1ie})^{-1}(-2\boldsymbol{K}\boldsymbol{v}_{1ie} - \boldsymbol{C}_1\boldsymbol{\sigma}(\boldsymbol{\Omega}_i))\Big] := \boldsymbol{\Phi}_i, \tag{38}$$

where $\boldsymbol{C}_1 = \mathrm{diag}(c_{11}, c_{12}, c_{13})$ with c_{11}, c_{12}, and c_{13} positive constants to be chosen later. It is noted that the matrix $(\boldsymbol{\Delta}_i + \boldsymbol{v}_{1ie}\star\boldsymbol{v}_{1ie})$ is invertible for all $\boldsymbol{v}_{1ie} \in \mathbb{R}^3$ since $\boldsymbol{\Delta}_i = \boldsymbol{I}_3 + \frac{1}{2}\boldsymbol{v}_{1ie}\star\boldsymbol{v}_{1ie}$, see (27).

Let Φ_{1i}, Φ_{2i}, and Φ_{3i} be the elements of $\boldsymbol{\Phi}_i$, i.e., $\boldsymbol{\Phi}_i = [\Phi_{1i}\ \Phi_{2i}\ \Phi_{3i}]^T$. From (38), we obtain the following bounds of $|\Phi_{1i}|$, $|\Phi_{2i}|$, and Φ_{3i}:

$$\begin{aligned}
|\Phi_{1i}| &\leq m_i\Big(\sup_{t\in\mathbb{R}^+}\|\ddot{\boldsymbol{\eta}}_{1id}(t)\| + k_1 + 2c_{11}\Big), \quad \Phi_{3i} \leq m_i\big(2g - \varrho + k_1 + 2c_{13}\big),\\
|\Phi_{2i}| &\leq m_i\Big(\sup_{t\in\mathbb{R}^+}\|\ddot{\boldsymbol{\eta}}_{1id}(t)\| + k_1 + 2c_{12}\Big), \quad \Phi_{3i} \geq m_i\big(\varrho - k_1 - 2c_{13}\big),
\end{aligned} \tag{39}$$

where we have used (8) and (9). We now specify the gain matrices $\boldsymbol{K}$ and $\boldsymbol{C}_1$ such that $\Phi_{3i} \geq \Phi^*_{3i}$ with Φ^*_{3i} being a strictly positive constant. From the last inequality in (39), it is seen that $\Phi_{3i} \geq \Phi_{3i}^{*}$ if we choose $\boldsymbol{K}$ and $\boldsymbol{C}_1$ such that

$$m_i\big(\varrho - k_1 - 2c_{13}\big) \geq \Phi_{3i}^{*}. \tag{40}$$

This condition is necessary for designing a smooth control law for α_{θ_i} later. We now solve (38) for f_i, α_{ϕ_i}, and α_{θ_i}. As such, the equation (38) yields

$$f_i \boldsymbol{e}_3 = \boldsymbol{R}_1^{-1}(\boldsymbol{\alpha}_{\boldsymbol{q}_i})\boldsymbol{\Phi}_i. \tag{41}$$

Since $\boldsymbol{R}_1^{-T}(\boldsymbol{\alpha}_{\boldsymbol{q}_i})\boldsymbol{R}_1^{-1}(\boldsymbol{\alpha}_{\boldsymbol{q}_i}) = \boldsymbol{I}_3$, we have

$$f_i = \sqrt{\boldsymbol{\Phi}_i^T\boldsymbol{\Phi}_i}. \tag{42}$$

On the other hand, using (23) and $\boldsymbol{e}_3 = [0\ 0\ 1]^T$ we can write (41) in a component form as follows:

$$\begin{aligned}
&\cos(\alpha_{\psi_i})\cos(\alpha_{\theta_i})\Phi_{1i} + \sin(\alpha_{\psi_i})\cos(\alpha_{\theta_i})\Phi_{2i} - \sin(\alpha_{\theta_i})\Phi_{3i} = 0,\\
&\big[-\sin(\alpha_{\psi_i})\cos(\alpha_{\phi_i}) + \sin(\alpha_{\phi_i})\sin(\alpha_{\theta_i})\cos(\alpha_{\psi_i})\big]\Phi_{1i} + \big[\cos(\alpha_{\psi_i})\cos(\alpha_{\phi_i}) + \sin(\alpha_{\phi_i})\sin(\alpha_{\theta_i})\sin(\alpha_{\psi_i})\big]\Phi_{2i} +\\
&\qquad \sin(\alpha_{\phi_i})\cos(\alpha_{\theta_i})\Phi_{3i} = 0,\\
&\big[\sin(\alpha_{\psi_i})\sin(\alpha_{\phi_i}) + \sin(\alpha_{\theta_i})\cos(\alpha_{\psi_i})\cos(\alpha_{\phi_i})\big]\Phi_{1i} + \big[-\cos(\alpha_{\psi_i})\sin(\alpha_{\phi_i}) + \sin(\alpha_{\theta_i})\sin(\alpha_{\psi_i})\cos(\alpha_{\phi_i})\big]\Phi_{2i} +\\
&\qquad \cos(\alpha_{\phi_i})\cos(\alpha_{\theta_i})\Phi_{3i} = f_i.
\end{aligned} \tag{43}$$

Now multiplying the second equation of (43) by $-\cos(\alpha_{\phi_i})$ then adding with the first equation of (43) multiplied by $\sin(\alpha_{\phi_i})$ results in

$$\alpha_{\phi_i} = \arcsin\left(\frac{\sin(\alpha_{\psi_i})\Phi_{1i} - \cos(\alpha_{\psi_i})\Phi_{2i}}{\sqrt{\boldsymbol{\Phi}_i^T\boldsymbol{\Phi}_i}}\right), \tag{44}$$

which is well defined since $|\sin(\alpha_{\psi_i})\Phi_{1i} - \cos(\alpha_{\psi_i})\Phi_{2i}| \leq \sqrt{\Phi_{1i}^2 + \Phi_{2i}^2} < \sqrt{\boldsymbol{\Phi}_i^T\boldsymbol{\Phi}_i}$ due to $\Phi_{3i} \geq \Phi_{3i}^{*} > 0$, see (40). Moreover, from the first equation of (43) we have

$$\alpha_{\theta_i} = \arctan\left(\frac{\cos(\alpha_{\psi_i})\Phi_{1i} + \sin(\alpha_{\psi_i})\Phi_{2i}}{\Phi_{3i}}\right), \tag{45}$$

which is also well defined since $\Phi_{3i} \geq \Phi_{3i}^{*} > 0$, see (40).

Remark 4.2: Since $\beta'_{ij} = 0, \forall \chi_{ij} \in [\chi_{ij}^{*}, \infty)$, see Property 1) of β_{ij} in (28), the control laws f_i, α_{ϕ_i}, and α_{θ_i} of the aircraft i depend only on its own states and the states of other neighbor aircraft if these aircraft are in a sphere, which is centered at the aircraft i and has a radius no greater than χ_{ijd} defined just below (29).

Substituting (38) into (37) results in

$$\dot{V}_1 \leq -\sum_{i=1}^{N}\boldsymbol{\Omega}_i^T\boldsymbol{C}_1\boldsymbol{\sigma}(\boldsymbol{\Omega}_i) + \sum_{i=1}^{N}\boldsymbol{\Omega}_i^T\frac{\sqrt{\boldsymbol{\Phi}_i^T\boldsymbol{\Phi}_i}}{m_i}\boldsymbol{H}(\boldsymbol{q}_{ie}, \boldsymbol{\alpha}_{\boldsymbol{q}_i})\boldsymbol{e}_3. \tag{46}$$

Substituting (38) into (25) results in

$$\dot{\boldsymbol{v}}_{1ie} = (\boldsymbol{\Delta}_i + \boldsymbol{v}_{1ie}\star\boldsymbol{v}_{1ie})^{-1}(-2\boldsymbol{K}\boldsymbol{v}_{1ie} - \boldsymbol{C}_1\boldsymbol{\sigma}(\boldsymbol{\Omega}_i)) + \frac{f_i}{m_i}\boldsymbol{H}(\boldsymbol{q}_{ie}, \boldsymbol{\alpha}_{\boldsymbol{q}_i})\boldsymbol{e}_3. \tag{47}$$

B. Stage 2

In this stage, we design the control $\boldsymbol{\tau}_i$ to stabilize $\boldsymbol{q}_{ie}$ at the origin. Before calculating $\dot{\boldsymbol{q}}_{ie}$, let us calculate $\dot{\boldsymbol{\alpha}}_{\boldsymbol{q}_i}$. From (24), we have

$$\dot{\boldsymbol{\alpha}}_{\boldsymbol{q}_i} = \boldsymbol{R}_2(\boldsymbol{\alpha}_{\boldsymbol{q}_i})\boldsymbol{\vartheta}_i, \tag{48}$$

where $\boldsymbol{R}_2(\bullet)$ is defined in (2), and

$$\begin{aligned}
\boldsymbol{\vartheta}_i = &\begin{bmatrix} 1 & 0 & -\sin(\alpha_{\theta_i}) \\ 0 & \cos(\alpha_{\phi_i}) & \cos(\alpha_{\theta_i})\sin(\alpha_{\phi_i}) \\ 0 & -\sin(\alpha_{\phi_i}) & \cos(\alpha_{\theta_i})\cos(\alpha_{\phi_i}) \end{bmatrix} \times \\
&\left[\frac{\partial\boldsymbol{\alpha}_{\boldsymbol{\eta}_{2i}}}{\partial\ddot{\boldsymbol{\eta}}_{1id}}\dddot{\boldsymbol{\eta}}_{1id} + \frac{\partial\boldsymbol{\alpha}_{\boldsymbol{\eta}_{2i}}}{\partial\psi_{id}}\dot{\psi}_{id} + \frac{\partial\boldsymbol{\alpha}_{\boldsymbol{\eta}_{2i}}}{\partial\boldsymbol{\eta}_{1ie}}\dot{\boldsymbol{\eta}}_{1ie} + \frac{\partial\boldsymbol{\alpha}_{\boldsymbol{\eta}_{2i}}}{\partial\boldsymbol{v}_{1ie}}\dot{\boldsymbol{v}}_{1ie} + \frac{\partial\boldsymbol{\alpha}_{\boldsymbol{\eta}_{2i}}}{\partial\boldsymbol{\Omega}_i}\sum_{j\in\mathbb{N}_i}\Big(\beta'_{ij}\dot{\boldsymbol{\eta}}_{1ij} + \beta''_{ij}\dot{\boldsymbol{\chi}}_{ij}\boldsymbol{\eta}_{1ij}\Big)\right].
\end{aligned} \tag{49}$$

Noticing all the derivatives $\dot{\boldsymbol{\eta}}_{1ie}$, $\dot{\boldsymbol{v}}_{1ie}$, $\dot{\boldsymbol{\eta}}_{1ij}$, and $\dot{\boldsymbol{\chi}}_{ij}$ are analytically available. Differentiating both sides of the last equation of (19) along the solutions of (48) and the third equation of (1) yields

$$\dot{\boldsymbol{q}}_{ie} = \boldsymbol{R}_2(\boldsymbol{q}_i)\boldsymbol{\omega}_i - \boldsymbol{R}_2(\boldsymbol{\alpha}_{\boldsymbol{q}_i})\boldsymbol{\vartheta}_i. \tag{50}$$

Since $\boldsymbol{q}_{ie} \in \mathbb{R}^4$ while $\boldsymbol{\omega}_i \in \mathbb{R}^3$ and $\boldsymbol{\tau}_i \in \mathbb{R}^3$, it is difficult to design the control $\boldsymbol{\tau}_i$ from (50) to stabilize $\boldsymbol{q}_{ie}$ at the origin. To overcome this difficulty, we perform the following coordinate transformations:

$$\begin{aligned} z_{0i} &= \alpha_{q_{0i}} q_{0i} + \boldsymbol{\alpha}_{\bar{\boldsymbol{q}}_i}^T \bar{\boldsymbol{q}}_i, \\ \bar{\boldsymbol{z}}_i &= \alpha_{q_{0i}} \bar{\boldsymbol{q}}_i - q_{0i}\boldsymbol{\alpha}_{\bar{\boldsymbol{q}}_i} - \boldsymbol{S}(\boldsymbol{\alpha}_{\bar{\boldsymbol{q}}_i})\bar{\boldsymbol{q}}_i, \end{aligned} \tag{51}$$

where $\alpha_{q_{0i}}$ is the first element of $\boldsymbol{\alpha}_{\boldsymbol{q}_i}$ and $\boldsymbol{\alpha}_{\bar{\boldsymbol{q}}_i}$ is the vector containing the second, third and fourth elements of $\boldsymbol{\alpha}_{\boldsymbol{q}_i}$, i.e.,

$$\boldsymbol{\alpha}_{\boldsymbol{q}_i} = [\alpha_{q_{0i}} \ \boldsymbol{\alpha}_{\bar{\boldsymbol{q}}_i}^T]^T. \tag{52}$$

Using (51), (52), and the third equation of (19), we have the following relationship between $(z_{0i}, \bar{\boldsymbol{z}}_i)$ and $\boldsymbol{q}_{ie}$:

$$\begin{bmatrix} z_{0i} - 1 \\ \bar{\boldsymbol{z}}_i \end{bmatrix} = \boldsymbol{Q}_i \boldsymbol{q}_{ie}, \tag{53}$$

where

$$\boldsymbol{Q}_i = -\begin{bmatrix} q_{0i} & q_{1i} & q_{2i} & q_{3i} \\ q_{1i} & -q_{0i} & q_{3i} & -q_{2i} \\ q_{2i} & -q_{3i} & -q_{0i} & q_{1i} \\ q_{3i} & q_{2i} & -q_{1i} & -q_{0i} \end{bmatrix}. \tag{54}$$

It is noted that the matrix $\boldsymbol{Q}_i$ is invertible because $\det(\boldsymbol{Q}_i) = -(q_{0i}^2 + q_{1i}^2 + q_{2i}^2 + q_{3i}^2) = -1$. Due to (53), the transformation (51) implies that designing the control $\boldsymbol{\tau}_i$ to stabilize $\boldsymbol{q}_{ie}$ at the origin is equivalent to designing $\boldsymbol{\omega}_i$ to stabilize z_{0i} at 1 and $\bar{\boldsymbol{z}}_i$ at the origin. Differentiating both sides of (51) along the solutions of the third equation of (1) and (48) yields

$$\begin{aligned} \dot{z}_{0i} &= -\frac{1}{2}\bar{\boldsymbol{z}}_i^T \boldsymbol{\omega}_{ie}, \\ \dot{\bar{\boldsymbol{z}}}_i &= \frac{1}{2}\boldsymbol{G}_i \boldsymbol{\omega}_{ie}, \end{aligned} \tag{55}$$

where

$$\begin{aligned} \boldsymbol{G}_i &= (z_{0i}\boldsymbol{I}_3 + \boldsymbol{S}(\bar{\boldsymbol{z}}_i)), \\ \boldsymbol{\omega}_{ie} &= \boldsymbol{\omega}_i - \boldsymbol{\vartheta}_i. \end{aligned} \tag{56}$$

Since the matrix $\boldsymbol{G}_i$ is not globally invertible, it is not an easy task to use the backstepping technique to design a virtual control for $\boldsymbol{\omega}_{ie}$ to stabilize $\bar{\boldsymbol{z}}_i$ at the origin and z_{0i} at 1. Therefore, we will construct a special Lyapunov function in conjunction with the function V_1 to directly design the moment vector $\boldsymbol{\tau}_i$. As such, differentiating both sides of the second equation of (56) along the solutions of the last equation of (1) gives

$$\dot{\boldsymbol{\omega}}_{ie} = \boldsymbol{\tau}_{ie}, \tag{57}$$

where we have chosen the control $\boldsymbol{\tau}_i$ as

$$\boldsymbol{\tau}_i = \boldsymbol{J}_i^{-1}\boldsymbol{S}(\boldsymbol{\omega}_i)\boldsymbol{J}_i\boldsymbol{\omega}_i + \boldsymbol{J}_i\big(\dot{\boldsymbol{\vartheta}}_i + \boldsymbol{\tau}_{ie}\big), \tag{58}$$

and $\boldsymbol{\tau}_{ie}$ is a new control to be designed. It is noted that $\dot{\boldsymbol{\vartheta}}_i$ is analytically obtained by differentiating $\boldsymbol{\vartheta}_i$, which is defined in (49). Before designing $\boldsymbol{\tau}_{ie}$, from the expression of the matrix $\boldsymbol{H}(\boldsymbol{q}_{ie}, \boldsymbol{\alpha}_{\boldsymbol{q}_i})$ in (21) and the relationship between $\boldsymbol{q}_{ie}$ and $(z_{0i}, \bar{\boldsymbol{z}}_i)$ defined in (53) we can write the term $\frac{1}{m_i}\sqrt{\boldsymbol{\Phi}_i^T\boldsymbol{\Phi}_i}\ \boldsymbol{\Omega}_i^T\boldsymbol{H}(\boldsymbol{q}_{ie}, \boldsymbol{\alpha}_{\boldsymbol{q}_i})e_3$ in the right hand side of (46) as

$$\frac{1}{m_i}\sqrt{\boldsymbol{\Phi}_i^T\boldsymbol{\Phi}_i}\ \boldsymbol{\Omega}_i^T\boldsymbol{H}(\boldsymbol{q}_{ie}, \boldsymbol{\alpha}_{\boldsymbol{q}_i})e_3 = \Psi_{0i}(z_{0i} - 1) + \overline{\boldsymbol{\Psi}}_i^T\bar{\boldsymbol{z}}_i \tag{59}$$

where Ψ_{0i} is a scalar function of, and $\overline{\boldsymbol{\Psi}}_i$ is a vector of functions of $\boldsymbol{\Omega}_i$, f_i, $\boldsymbol{q}_{ie}$, and $\boldsymbol{\alpha}_{\boldsymbol{q}_i}$. Now, to design the control $\boldsymbol{\tau}_{ie}$, we consider the following Lyapunov function candidate:

$$V_2 = V_1 + \sum_{i=1}^{N}\Big((z_{0i} - 1)^2 + \|\bar{\boldsymbol{z}}_i\|^2 + \frac{1}{2}\tilde{\boldsymbol{\omega}}_i^T\boldsymbol{\Gamma}_i^{-1}\tilde{\boldsymbol{\omega}}_i\Big), \tag{60}$$

where $\boldsymbol{\Gamma}_i$ is a positive definite matrix, and

$$\begin{aligned}\tilde{\boldsymbol{\omega}}_i &= \boldsymbol{\omega}_{ie} - \overline{\boldsymbol{\omega}}_i,\\ \overline{\boldsymbol{\omega}}_i &= -\Big(\frac{1}{2}(\Psi_{0i}^2+1)+c_{2i}\Big)\bar{\boldsymbol{z}}_i - \overline{\boldsymbol{\Psi}}_i,\end{aligned} \tag{61}$$

with c_{2i} being a positive constant. Differentiating both sides of (60) along the solutions of (46), (55) and using (59) results in

$$\dot{V}_2 \le -\sum_{i=1}^{N}\boldsymbol{\Omega}_i^T\boldsymbol{C}_1\boldsymbol{\sigma}(\boldsymbol{\Omega}_i) + \sum_{i=1}^{N}\Big(\Psi_{0i}(z_{0i}-1) + \overline{\boldsymbol{\Psi}}_i^T\bar{\boldsymbol{z}}_i + \bar{\boldsymbol{z}}_i^T\boldsymbol{\omega}_{ie} + \tilde{\boldsymbol{\omega}}_i^T\boldsymbol{\Gamma}_i^{-1}(\boldsymbol{\tau}_{ie} - \dot{\overline{\boldsymbol{\omega}}}_i)\Big), \tag{62}$$

which suggests that we choose

$$\boldsymbol{\tau}_{ie} = \dot{\overline{\boldsymbol{\omega}}}_i - \boldsymbol{\Gamma}_i^2\tilde{\boldsymbol{\omega}}_i - \boldsymbol{\Gamma}_i\bar{\boldsymbol{z}}_i. \tag{63}$$

Note that $\dot{\overline{\boldsymbol{\omega}}}_i$ can be obtained analytically by differentiating $\overline{\boldsymbol{\omega}}_i$ given in (61). The control $\boldsymbol{\tau}_i$ is found by substituting (63) into (58). Similar to Remark 4.2, we have the following remark:

Remark 4.3: By construction, the control $\boldsymbol{\tau}_i$ of the aircraft i depend only on its own states and the states of other neighbor aircraft if these aircraft are in a sphere, which is centered at the aircraft i and has a radius no greater than χ_{ijd} defined just below (29) because outside this sphere $\beta_{ij}=0$, $\beta'_{ij}=0$, $\beta''_{ij}=0$, and $\beta'''_{ij}=0$, see Property 1) of β_{ij} in (28).

Substituting (63) into (62) gives

$$\dot{V}_2 \le -\sum_{i=1}^{N}\boldsymbol{\Omega}_i^T\boldsymbol{C}_1\boldsymbol{\sigma}(\boldsymbol{\Omega}_i) - \sum_{i=1}^{N}\tilde{\boldsymbol{\omega}}_i^T\boldsymbol{\Gamma}_i\tilde{\boldsymbol{\omega}}_i - \sum_{i=1}^{N}\Big[\Big(\frac{1}{2}(\Psi_{0i}^2+1)+c_{2i}\Big)\|\bar{\boldsymbol{z}}_i\|^2 - \Psi_{0i}(z_{0i}-1)\Big]. \tag{64}$$

Since $\|\bar{\boldsymbol{z}}_i\|^2 = 1 - z_{0i}^2 \ge 1 - z_{0i}$ and $|\Psi_{0i}| \le \frac{1}{2}(\Psi_{0i}^2+1)$, we can write (64) as

$$\dot{V}_2 \le -\sum_{i=1}^{N}\Big(\boldsymbol{\Omega}_i^T\boldsymbol{C}_1\boldsymbol{\sigma}(\boldsymbol{\Omega}_i) + \tilde{\boldsymbol{\omega}}_i^T\boldsymbol{\Gamma}_i\tilde{\boldsymbol{\omega}}_i + c_{2i}\|\bar{\boldsymbol{z}}_i\|^2\Big). \tag{65}$$

From the above control design, we have the following closed-loop system:

$$\begin{aligned}\dot{\boldsymbol{\eta}}_{1ie} &= \boldsymbol{v}_{1ie},\\ \dot{\boldsymbol{v}}_{1ie} &= (\boldsymbol{\Delta}_i + \boldsymbol{v}_{1ie}\star\boldsymbol{v}_{1ie})^{-1}(-2\boldsymbol{K}\boldsymbol{v}_{1ie} - \boldsymbol{C}_1\boldsymbol{\sigma}(\boldsymbol{\Omega}_i)) + \frac{1}{m_i}\sqrt{\boldsymbol{\Phi}_i^T\boldsymbol{\Phi}_i}\boldsymbol{H}(\boldsymbol{q}_{ie},\boldsymbol{\alpha}_{\boldsymbol{q}_i})\boldsymbol{e}_3,\\ \dot{\boldsymbol{q}}_{ie} &= \boldsymbol{R}_2(\boldsymbol{q}_i)\boldsymbol{\omega}_i - \boldsymbol{R}_2(\boldsymbol{\alpha}_{\boldsymbol{q}_i})\boldsymbol{\vartheta}_i,\\ \dot{\boldsymbol{\omega}}_{ie} &= \dot{\overline{\boldsymbol{\omega}}}_i - \boldsymbol{\Gamma}_i^2\tilde{\boldsymbol{\omega}}_i - \boldsymbol{\Gamma}_i\bar{\boldsymbol{z}}_i.\end{aligned} \tag{66}$$

The control design has been completed. We summarize the results in the following theorem.

Theorem 4.1: Under Assumption 2.1, the coordination control laws consisting of (42) and (58) for the aircraft i solve Coordination Control Objective 2.1 provided that the gain matrices $\boldsymbol{K}$ and $\boldsymbol{C}_1$ are chosen such that the condition (40) holds. In particular, the following results hold under Assumption 2.1:

1) The actual control input f_{il}, $l=1,\cdots,4$ to the rotor l of the aircraft i can be found by solving (3) with f_i and $\boldsymbol{\tau}_i$ given in (42) and (58), respectively, i.e.,

$$\begin{bmatrix} f_{i1}\\ f_{i2}\\ f_{i3}\\ f_{i4}\end{bmatrix} = \begin{bmatrix} 1 & 1 & 1 & 1\\ 0 & -L_i & 0 & L_i\\ -L_i & 0 & L_i & 0\\ -E_{ia} & E_{ia} & -E_{ia} & E_{ia}\end{bmatrix}^{-1}\begin{bmatrix} f_i\\ \boldsymbol{\tau}_i\end{bmatrix}. \tag{67}$$

2) There is no collision between any aircraft and the closed-loop system (66) is forward complete.
3) The position vector $\boldsymbol{\eta}_{1i}(t)$ and the yaw angle $\psi_i(t)$ of the aircraft i almost globally asymptotically and locally exponentially track their reference trajectories $\boldsymbol{\eta}_{1id}(t)$ and $\psi_{id}(t)$, respectively, i.e., $\lim_{t\to\infty}(\boldsymbol{\eta}_{1i}(t) - \boldsymbol{\eta}_{1id}(t)) = 0$ and $\lim_{t\to\infty}(\psi_i(t) - \psi_{id}(t)) = 0$.
4) All other states of the aircraft dynamics are bounded.

Proof. See Appendix B.

V. SIMULATION RESULTS

In this section, we illustrate the effectiveness of the proposed coordination control design through a numerical simulation on a group of $N = 6$ identical quadrotor aircraft. The aircraft's parameters are taken as $m_i = 0.5$kg, $L_i = 0.25$m, $E_{ia} = 0.05$m, $g = 9.81\text{m}/s^2$, and $\boldsymbol{J}_i = 10^{-3}\text{diag}(5,5,9)\text{kg/m}^2$. The initial conditions are taken as

$$\boldsymbol{\eta}_{1i}(0) = R_0\boldsymbol{l}_i + [0\ 0\ 2R_0]^T,\ \boldsymbol{v}_{1i}(0) = [0\ 0\ 0]^T,\ \boldsymbol{\omega}_i(0) = [0\ 0\ 0]^T, \tag{68}$$

where $R_0 = 25$m, $\boldsymbol{l}_1 = [1\ 0\ 0]^T$, $\boldsymbol{l}_2 = [0\ 1\ 0]^T$, $\boldsymbol{l}_3 = [-1\ 0\ 0]^T$, $\boldsymbol{l}_4 = [0\ -1\ 0]^T$, $\boldsymbol{l}_5 = [0\ 0\ 1]^T$, $\boldsymbol{l}_6 = [0\ 0\ -1]^T$. The initial values of $\boldsymbol{q}_i(0)$ are chosen such that $[\phi_i(0), \theta_i(0), \psi_i(0)] = [4,-4,1]\frac{\pi}{6i}$, $i = 1,...,N$.

The above initial conditions mean that the aircraft are uniformly distributed on a sphere centered at $(0,0,2R_0)$ at the initial time. We choose the above initial values of the roll and pitch angles, $\phi_i(0)$ and $\theta_i(0)$, to illustrate the capacity of the proposed coordination control design in handling large roll and pitch angles at the initial time. Since the initial value of the pitch angle of the aircraft 1 is $-2\pi/3$, the choice of the above initial values is also to demonstrate the fact that the proposed coordination control design can avoid singularities. This is because the pitch angle of the aircraft 1 will converge to zero from its initial value of $-2\pi/3$. The reference trajectories are taken as

$$\boldsymbol{\eta}_{1id}(t) = -R_0\boldsymbol{l}_i + \begin{bmatrix} 0 \\ 0 \\ 2R_0 \end{bmatrix}, \forall\, 0 \le t \le 40,\ \boldsymbol{\eta}_{1id}(t) = \begin{bmatrix} R_0\sin(0.05(t-40)) \\ R_0\cos(0.05(t-40)) \\ 0.5(t-40) \end{bmatrix} + \begin{bmatrix} 0 \\ -R_0 \\ 2R_0 \end{bmatrix},\ \forall\, 40 < t \le 180. \tag{69}$$

The purpose of choosing the initial conditions (68) and the reference trajectories (69) is to illustrate both collision avoidance and reference trajectory tracking capacities of the proposed coordination control design. With the above initial conditions and the reference trajectories, all the aircraft need to cross the point $(0,0,2R_0)$, i.e., the center of the aforementioned sphere. This is an effective illustration of the collision avoidance capacity of the proposed coordination controller. The control gains d_{ij}, a_{ij}, b_{ij}, $\boldsymbol{K}$, $\boldsymbol{C}_1$, c_{2i}, and $\boldsymbol{\Gamma}_i$ need to be chosen such that the conditions (32) and (40) hold. Since these conditions are independent from d_{ij}, c_{2i}, and $\boldsymbol{\Gamma}_i$, an easy way to choose a_{ij}, b_{ij}, $\boldsymbol{K}$, and $\boldsymbol{C}_1$ that satisfy the above conditions is given in the following steps:

1) Choose the positive constant ϱ such that it satisfies the condition (9). In this step, it is necessary to calculate $\sup_{t\in\mathbb{R}^+}|\ddot{z}_{id}(t)|$ because it appears in the condition (9).
2) Choose the positive definite matrices $\boldsymbol{K}$ and $\boldsymbol{C}_1$ such that they satisfy the condition (40).
3) Choose the constants a_{ij} and b_{ij} such that they satisfy the condition (32). This step requires a calculation of $\chi_{ijd} = \boldsymbol{\eta}_{1ijd}^T\boldsymbol{K}\boldsymbol{\eta}_{1ijd}$, see (30). Since $\chi_{ijd} \ge \lambda_{\min}(\boldsymbol{K})\|\boldsymbol{\eta}_{1ijd}\|^2$, a simple practice is to choose the same a_{ij} and b_{ij} for all $(i,j) \in \mathbb{N}$, $j \ne i$ by taking $\chi_{ij}^* = \lambda_{\min}(\boldsymbol{K})\inf_{t\in\mathbb{R}^+}\|\boldsymbol{\eta}_{1ijd}(t)\|^2$.

The rule of thumbs is that the larger value of the control gains results in a faster response and larger repulsive forces but a larger control effort. Moreover, a_{ij} should not be chosen too close to b_{ij} because such as choice will result in a large change of the smooth step function $h(\chi_{ij}, a_{ij}, b_{ij})$ from 0 to 1 when χ_{ij} increases from a_{ij} to b_{ij}. This results in a large derivation of β'_{ij}, β''_{ij}, and β'''_{ij} when χ_{ij} increases from a_{ij} to b_{ij}.

Since the specified reference trajectories (69) give $\sup_{t\in\mathbb{R}^+}|\ddot{z}_{id}(t)| = 0$ and $\inf_{t\in\mathbb{R}^+}\|\boldsymbol{\eta}_{1ijd}(t)\|^2 = 2R_0^2$, by applying the above steps we can choose the control gains as $d_{ij} = 1$, $a_{ij} = 75$, $b_{ij} = 140$, for all $(i,j) \in \mathbb{N}$, $\boldsymbol{K} = \text{diag}(0.25, 0.25, 0.25)$, $\boldsymbol{C}_1 = \text{diag}(0.5, 0.5, 0.5)$, $c_{2i} = 2$, and $\boldsymbol{\Gamma}_i = \text{diag}(5,5,5)$, for all $i = 1,...,N$. Simulation results are plotted in Fig. 1, Fig. 2, and Fig. 3. The position trajectories of the aircraft are plotted in Fig. 1, where the red circles represent the initial positions while the red and blue circular disks represent the positions at $t = 40s$ and at the finial positions at $t = 180s$ of the aircraft. Fig. 2.A plots the normalized value of product of all the relative distances between the aircraft $d_a = \left(\prod_{(i,j)\in\mathbb{N}, i\ne j}\|\boldsymbol{\eta}_{1ij}(t)\|\right)^{\frac{1}{24}}$, which is always larger than zero for all $0 \le t \le 180$. This means that there is no collision between any aircraft. Fig. 2.B plots the control forces f_{il}, $i = 1,...,N$ and $l = 1,...,4$. Fig. 2.C and Fig. 2.D plot the position and attitude tracking errors. Noticing that an sudden change in control inputs and tracking errors at $t = 40s$ due to a change of the reference trajectories at $t = 40s$. It is seen from these figures that all tracking errors asymptotically converge to zero. Noticing that it takes longer time for the position tracking error vector $\boldsymbol{\eta}_{1ie}(t)$ to converge to zero than for the attitude tracking error vector $\boldsymbol{q}_{ie}(t)$ since we need to choose sufficiently small gain matrices $\boldsymbol{K}$ and $\boldsymbol{C}_1$ so that the conditions (40) holds. Fig. 3.A plots the "repulsive forces", $\boldsymbol{\Omega}_i^{Re}$, without bounding by the saturation function $\boldsymbol{\sigma}(\bullet)$, i.e., $\boldsymbol{\Omega}_i^{Re} = -\sum_{j\in\mathbb{N}_i}\beta'_{ij}\boldsymbol{\eta}_{1ij}$. We see from Fig. 3.A that the repulsive forces are only active (nonzero) for the first 22 second, i.e., when the quadrotors are sufficiently close to each other. Fig. 3.B, Fig. 3.C, and Fig. 3.D plot the roll, pitch, and yaw angles. It is seen from Fig. 3.C that the proposed coordination control design can avoid a singularity when the pitch angle of the aircraft 1 is equal to $-\pi/2$. This is because the pitch angle of the aircraft 1 converges smoothly to zero from its initial value of $-2\pi/3$. Finally, local exponential convergence of the tracking errors can be seen from the magnified plots in Figs. 2.C, 2.D, 3.B, 3.C, and 3.D.

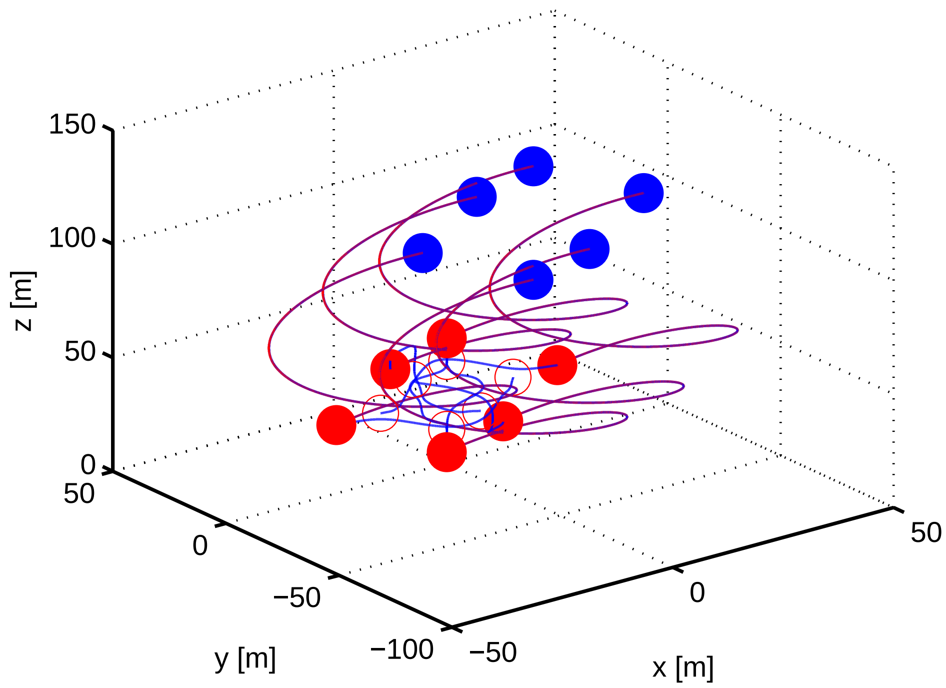

Fig. 1. Trajectories of the aircraft.

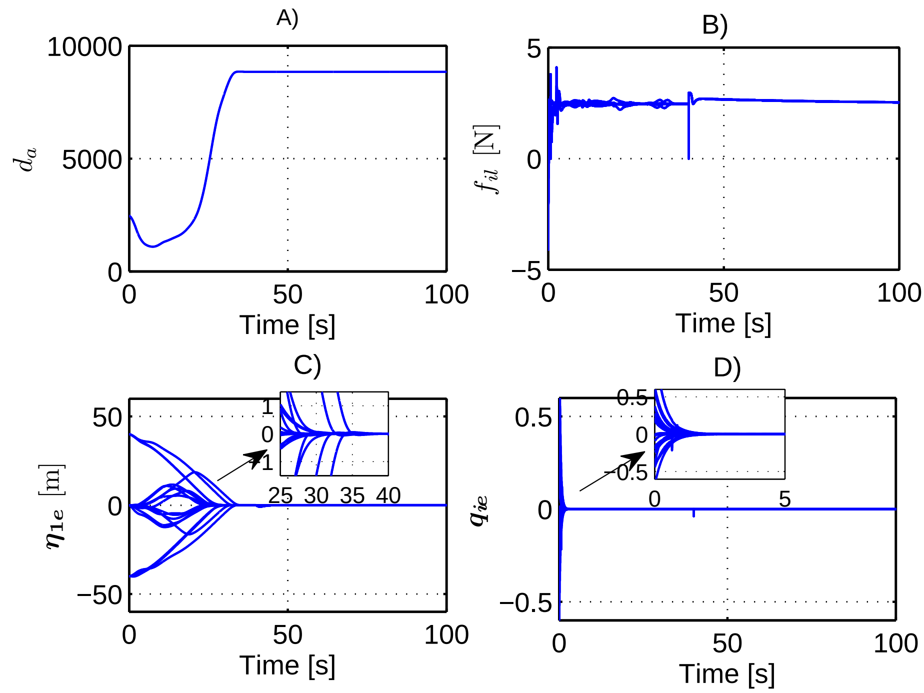

Fig. 2. A) Normalized value of relative distances, B) control inputs, C) Position tracking errors, D) Attitude tracking errors.

VI. Conclusions

Distributed coordination controllers for a group of N quadrotor VTOL aircraft in three-dimensional space have been designed. The controllers guaranteed no collision between any aircraft and an asymptotic convergence of tracking errors to zero. The attractive points of this paper include the combination of the Euler angles and unit-quaternion for the aircraft's attitude representation in Subsections II-A and IV-A1, the new bounded control design technique for second-order systems in Subsection III-B, the non-zero convergent result in Subsection III-C, pairwise collision avoidance functions in Subsection IV-A2, and the technique to design the moment vector in Subsection IV-B . An extension of the proposed coordination control design to underwater vehicles is under consideration.

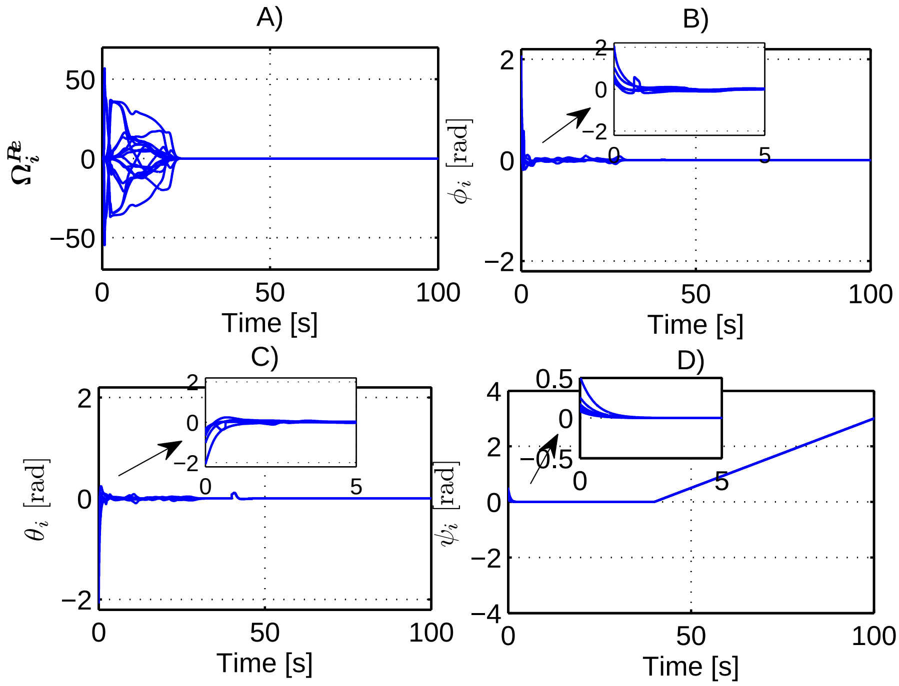

Fig. 3. A) Repulsive forces between quadrotors, B) Roll angles, C) Pitch angles, D) Yaw angles.

ACKNOWLEDGMENTS

The author would like to express his sincere gratitude to the Associate Editor and the reviewers for their helpful comments.

APPENDIX A
PROOF OF LEMMA 3.2

Consider the following function

$$V = \frac{1}{2}\|\boldsymbol{x}_{12}\|^2 \tag{70}$$

whose derivative satisfies

$$\dot{V} = \boldsymbol{x}_{12}^T\dot{\boldsymbol{x}}_{12}. \tag{71}$$

Adding and subtracting $\boldsymbol{x}_{12}^T\big(\boldsymbol{B}\boldsymbol{x}_{12} + \frac{1}{2}(\dot{\boldsymbol{x}}_1 - \boldsymbol{\mu})\star(\dot{\boldsymbol{x}}_1 - \boldsymbol{\mu})(\dot{\boldsymbol{x}}_1 - \boldsymbol{\mu}) - \frac{1}{2}(\dot{\boldsymbol{x}}_2 - \boldsymbol{\mu})\star(\dot{\boldsymbol{x}}_2 - \boldsymbol{\mu}))(\dot{\boldsymbol{x}}_2 - \boldsymbol{\mu})\big)$ to the right hand side of (71) result in

$$\begin{aligned}\dot{V} =& \boldsymbol{x}_{12}^T\Big[\Big(\boldsymbol{I}_{n\times n} + \frac{1}{2}(\dot{\boldsymbol{x}}_1 - \boldsymbol{\mu})\star(\dot{\boldsymbol{x}}_1 - \boldsymbol{\mu})\Big)(\dot{\boldsymbol{x}}_1 - \boldsymbol{\mu}) - \Big(\boldsymbol{I}_{n\times n} + \frac{1}{2}(\dot{\boldsymbol{x}}_2 - \boldsymbol{\mu})\star(\dot{\boldsymbol{x}}_2 - \boldsymbol{\mu})\Big)(\dot{\boldsymbol{x}}_2 - \boldsymbol{\mu}) + \boldsymbol{B}\boldsymbol{x}_{12}\Big] - \\ & \boldsymbol{x}_{12}^T\boldsymbol{B}\boldsymbol{x}_{12} - \frac{1}{2}\boldsymbol{x}_{12}^T\boldsymbol{A}\dot{\boldsymbol{x}}_{12},\end{aligned} \tag{72}$$

where $\boldsymbol{A} = \mathrm{diag}((\dot{x}_{11} - \mu_1)^2 + (\dot{x}_{11} - \mu_1)(\dot{x}_{21} - \mu_1) + (\dot{x}_{21} - \mu_1)^2,\ (\dot{x}_{12} - \mu_2)^2 + (\dot{x}_{12} - \mu_2)(\dot{x}_{22} - \mu_2) + (\dot{x}_{22} - \mu_2)^2, ..., (\dot{x}_{1n} - \mu_n)^2 + (\dot{x}_{1n} - \mu_n)(\dot{x}_{2n} - \mu_n) + (\dot{x}_{2n} - \mu_n)^2)$, with $\dot{x}_{11}, \dot{x}_{12}, ..., \dot{x}_{1n}$ are elements of the vector $\dot{\boldsymbol{x}}_1$, i.e., $\dot{\boldsymbol{x}}_1 = [\dot{x}_{11},\ \dot{x}_{12}, ..., \dot{x}_{1n}]^T$; $\dot{x}_{21}, \dot{x}_{22}, ..., \dot{x}_{2n}$ are elements of the vector $\dot{\boldsymbol{x}}_2$, i.e., $\dot{\boldsymbol{x}}_2 = [\dot{x}_{21},\ \dot{x}_{22}, ..., \dot{x}_{2n}]^T$; and $\mu_1, \mu_2, ..., \mu_n$ are elements of $\boldsymbol{\mu}$, i.e., $\boldsymbol{\mu} = [\mu_1, \mu_2, ..., \mu_n]^T$. It is seen that the matrix $\boldsymbol{A}$ is diagonal and nonnegative definite. Now using the second condition in (14), we can write (72) as

$$\dot{V} \geq -\boldsymbol{x}_{12}^T\boldsymbol{B}\boldsymbol{x}_{12} - \frac{1}{2}\boldsymbol{x}_{12}^T\boldsymbol{A}\dot{\boldsymbol{x}}_{12} + a. \tag{73}$$

Let us consider the term $\boldsymbol{x}_{12}^T\boldsymbol{A}\dot{\boldsymbol{x}}_{12}$. This term must satisfy one of the following two conditions: 1) $\boldsymbol{x}_{12}^T\boldsymbol{A}\dot{\boldsymbol{x}}_{12} \leq 0$ and 2) $\boldsymbol{x}_{12}^T\boldsymbol{A}\dot{\boldsymbol{x}}_{12} > 0$. We define a sequence of points $t_i, i = 0, 1, \cdots$ on the time axis such that $t_i < t_{i+1}$. Now, let us consider each interval as follows.

First, Condition 1) holds in the interval $[t_0, t_1]$ and Condition 2) holds in the interval $(t_1, t_2]$. In the interval $[t_0, t_1]$, substituting $\boldsymbol{x}_{12}^T\boldsymbol{A}\dot{\boldsymbol{x}}_{12} \leq 0$ into (73) yields

$$\dot{V} \geq -\boldsymbol{x}_{12}^T\boldsymbol{B}\boldsymbol{x}_{12} + a. \tag{74}$$

Therefore, we have

$$V(t) \geq \left(V(t_0) - \frac{a}{2\lambda_M(\boldsymbol{B})}\right)e^{-2\lambda_M(\boldsymbol{B})(t-t_0)} + \frac{a}{2\lambda_M(\boldsymbol{B})} \quad \Rightarrow \quad V(t) \geq \min\left(V(t_0), \frac{a}{2\lambda_M(\boldsymbol{B})}\right) \tag{75}$$

for all $t_0 \leq t \leq t_1$. Substituting $V(t) = \frac{1}{2}\|\boldsymbol{x}_1(t) - \boldsymbol{x}_2(t)\|^2$, $V(t_0) = \frac{1}{2}\|\boldsymbol{x}_1(t_0) - \boldsymbol{x}_2(t_0)\|^2$, see (70), and the first condition specified in (14) into (75) results in (15) in the interval $t_0 \leq t \leq t_1$.

In the interval $(t_1, t_2]$, since $\boldsymbol{x}_{12}^T\boldsymbol{A}\dot{\boldsymbol{x}}_{12} > 0$ and $\boldsymbol{A}$ is diagonal and nonnegative definite matrix, there exists a diagonal and nonnegative definite matrix $\boldsymbol{Q}$, whose elements can be functions of t, $\dot{\boldsymbol{x}}_1 - \boldsymbol{\mu}$, and $\dot{\boldsymbol{x}}_2 - \boldsymbol{\mu}$, such that

$$\boldsymbol{A}\dot{\boldsymbol{x}}_{12} = \boldsymbol{Q}\boldsymbol{x}_{12}. \tag{76}$$

Since the matrices $\boldsymbol{A}$ and $\boldsymbol{Q}$ are nonnegative definite, the system (76) is unstable. Hence, $\|\boldsymbol{x}_{12}(t)\| \geq \|\boldsymbol{x}_{12}(t_0)\|$. This means from the first condition specified in (14) that $\|\boldsymbol{x}_{12}(t)\| > a_0$ in the interval $(t_1, t_2]$. Hence, we have proved that (15) holds in the interval $[t_0, t_2]$.

Second, Condition 2) holds in the interval $[t_0, t_1]$ and Condition 1) holds in the interval $(t_1, t_2]$. Carrying out the same analysis as above, we have $\|\boldsymbol{x}_{12}(t)\| > a_0$ for all $t_0 \leq t \leq t_1$ and (15) holds in the interval $(t_1, t_2]$. This means that (15) holds in the interval $[t_0, t_2]$ as well. Repeating the above procedure for the intervals $(t_2, t_3]$ and $(t_3, t_4]$ with a note that $\|\boldsymbol{x}_{12}(t_2)\| \geq \min\left(a_0, \sqrt{\frac{a}{\lambda_M(\boldsymbol{B})}}\right)$, and other intervals results in (15) for all $t \geq t_0 \geq 0$. □

APPENDIX B
PROOF OF THEOREM 4.1

A. Proof of no collisions and complete forwardness of the closed-loop system

It is seen from (65) that $\dot{V}_2 \leq 0$. Integrating $\dot{V}_2 \leq 0$ from t_0 to t and using the definition of V_2 in (60), where V_1 is defined in (33), result in

$$V_2(t) \leq V_2(t_0), \tag{77}$$

where

$$V_2(t) = \frac{1}{2}\left(\sum_{i=1}^{N}\|2\boldsymbol{K}\boldsymbol{\eta}_{1ie}(t) + \boldsymbol{\Delta}_i(t)\boldsymbol{v}_{1ie}(t)\|^2 + \sum_{i=1}^{N}\sum_{j\in\mathbb{N}_i}\beta_{ij}(t)\right) + \sum_{i=1}^{N}\left((z_{0i}(t)-1)^2 + \|\bar{\boldsymbol{z}}_i(t)\|^2 + \frac{1}{2}\tilde{\boldsymbol{\omega}}_i^T(t)\boldsymbol{\Gamma}_i^{-1}\tilde{\boldsymbol{\omega}}_i(t)\right) \tag{78}$$

and $V_2(t_0) = V_2(t)|_{t=t_0}$, for all $t \geq t_0 \geq 0$. The initial condition (6) in Assumption 2.1 and Properties 2) and 3) of β_{ij} in (28) imply that the right hand side of (77) is bounded by a positive constant depending on the initial conditions. Boundedness of the right hand side of (77) implies that the left hand side of (77) must be also bounded. As a result, $\beta_{ij}(\chi_{ij})$, where χ_{ij} is defined in (26), must be smaller than some positive constant depending on the initial conditions for all $t \geq t_0 \geq 0$. Since $\beta_{ij}(\chi_{ij})$ is a smooth function of χ_{ij}, which is a smooth function of $\boldsymbol{\eta}_{1ij}$, $\boldsymbol{v}_{1ie}$, and $\boldsymbol{v}_{1je}$, and at the initial time t_0 we have $\chi_{ij}(t_0) \geq \varepsilon_{12}$, see Condition (6), we have $\chi_{ij}(t)$ must be larger than some positive constant depending on the initial conditions and the choice of the function β_{ij}. For example, if the function β_{ij} is chosen as in (31), we then have $\chi_{ij}(t) > a_{ij}$ with a_{ij} defined in (32) for all $(i,j) \in \mathbb{N}$, $i \neq j$ and for all $t \geq t_0 \geq 0$, i.e., from definition of χ_{ij} in (26) we must have

$$\boldsymbol{\eta}_{1ij}(t)^T\left(\boldsymbol{K}\boldsymbol{\eta}_{1ij}(t) + \boldsymbol{\Delta}_i(t)\boldsymbol{v}_{1ie}(t) - \boldsymbol{\Delta}_j(t)\boldsymbol{v}_{1je}(t)\right) \geq \varepsilon_{12},\ \forall t \geq t_0 \geq 0, \tag{79}$$

where $\varepsilon_{12} > a_{ij}$. Applying Lemma 3.2 with $\boldsymbol{x}_1 = \boldsymbol{\eta}_{1i}$, $\boldsymbol{x}_2 = \boldsymbol{\eta}_{1j}$, and $\boldsymbol{\mu}(t) = \dot{\boldsymbol{\eta}}_{od}$ gives $\boldsymbol{\eta}_{1ij}(t) \geq \min\left(\varepsilon_{11}, \sqrt{\frac{\varepsilon_{12}}{\lambda_M(\boldsymbol{K})}}\right) := \varepsilon_3$ for all $t \geq t_0 \geq 0$. This means that there is no collision between any aircraft for all $t \geq t_0 \geq 0$.

Boundedness of $V_2(t)$ for all $\geq t_0 \geq 0$ implies that of $2\boldsymbol{K}\boldsymbol{\eta}_{1ie}(t) + \boldsymbol{\Delta}_i(t)\boldsymbol{v}_{1ie}(t)$, $\beta_{ij}(t)$, $z_{0i}(t)$, $\bar{\boldsymbol{z}}_i(t)$, and $\tilde{\boldsymbol{\omega}}_i(t)$. Since $2\boldsymbol{K}\boldsymbol{\eta}_{1ie}(t) + \boldsymbol{\Delta}_i(t)\boldsymbol{v}_{1ie}(t)$ is bounded, it is not difficult to show that $\boldsymbol{\eta}_{1ie}(t)$ and $\boldsymbol{v}_{1ie}(t)$ are bounded due to $\boldsymbol{\Delta}_i(t)$ defined in (27). Moreover, boundedness of $\boldsymbol{\eta}_{1ie}(t)$, $\boldsymbol{v}_{1ie}(t)$, $\beta_{ij}(t)$, $z_{0i}(t)$, $\bar{\boldsymbol{z}}_i(t)$, and $\tilde{\boldsymbol{\omega}}_i(t)$ implies by construction that $\boldsymbol{\omega}_{ie}(t)$ is bounded. Therefore, the closed-loop system (66) is forward complete due to boundedness of the above signals and reference signals $(\boldsymbol{\eta}_{1id}(t), \psi_{id}(t))$ and their derivatives assumed in Assumption 2.1.

B. Equilibrium set

We use Lemma 3.4 to find the equilibrium set, which the trajectories of the closed-loop system (66) tend to. Integrating both sides of (65) gives $\int_0^\infty \varpi(t)dt \leq V_2(t_0)$, where $\varpi(t) = \sum_{i=1}^N \varpi_i(t)$ with $\varpi_i(t) = \big(\boldsymbol{\Omega}_i^T(t)\boldsymbol{C}_1\boldsymbol{\sigma}(\boldsymbol{\Omega}_i(t)) + \tilde{\boldsymbol{\omega}}_i^T(t)\boldsymbol{\Gamma}_i\tilde{\boldsymbol{\omega}}_i(t) + c_{2i}\|\bar{\boldsymbol{z}}_i(t)\|^2\big)$. The function $\varpi(t)$ is scalar, nonnegative and differentiable. The derivative of $\varpi(t)$ along the solutions of the closed-loop system (66) using Properties of the function β_{ij} in (28) satisfies $\big|\frac{\mathrm{d}\varpi(t)}{\mathrm{d}t}\big| \leq M\varpi(t)$ with M a positive constant. Therefore, Lemma 3.4 results in $\lim_{t\to\infty}\varpi(t) = 0$, which means that $\lim_{t\to\infty}\varpi_i(t) = 0$, i.e.,

$$\lim_{t\to\infty}\Big(\boldsymbol{\Omega}_i^T(t)\boldsymbol{C}_1\boldsymbol{\sigma}(\boldsymbol{\Omega}_i(t)) + \tilde{\boldsymbol{\omega}}_i^T(t)\boldsymbol{\Gamma}_i\tilde{\boldsymbol{\omega}}_i(t) + c_{2i}\|\bar{\boldsymbol{z}}_i(t)\|^2\Big) = 0. \tag{80}$$

This limit yields

$$\begin{cases} \lim_{t\to\infty}\boldsymbol{\Omega}_i(t) = 0, \\ \lim_{t\to\infty}\tilde{\boldsymbol{\omega}}_i(t) = 0, \\ \lim_{t\to\infty}\bar{\boldsymbol{z}}_i(t) = 0, \end{cases} \Rightarrow \begin{cases} \lim_{t\to\infty}\boldsymbol{\Omega}_i(t) = 0, \\ \lim_{t\to\infty}\boldsymbol{\omega}_{ie}(t) = 0, \\ \lim_{t\to\infty}\boldsymbol{q}_{ie}(t) = 0, \end{cases} \tag{81}$$

where we have used the following implications:

$$\begin{aligned} &\lim_{t\to\infty}\boldsymbol{\Omega}_i(t) = 0 \quad \Rightarrow \begin{cases} \lim_{t\to\infty}\Psi_{0i}(t) = 0, \\ \lim_{t\to\infty}\overline{\boldsymbol{\Psi}}_i(t) = 0, \end{cases} \\ &\lim_{t\to\infty}\bar{\boldsymbol{z}}_i(t) = 0 \quad \Rightarrow \lim_{t\to\infty} z_{0i}(t) = 1 \quad \Rightarrow \lim_{t\to\infty}\boldsymbol{q}_{ie}(t) = 0, \end{aligned} \tag{82}$$

which are resulted from (59), (53), and $z_{0i}^2 + \|\bar{\boldsymbol{z}}_i\|^2 = 1$.

The limit $\lim_{t\to\infty}\boldsymbol{q}_{ie}(t) = 0$ implies that $\lim_{t\to\infty}(\psi_i(t) - \psi_{id}(t)) = 0$. We now need to show that $\lim_{t\to\infty}\boldsymbol{\eta}_{1ie}(t) = 0$. Since we have already proven that $\boldsymbol{\eta}_{1ie}(t)$ and $\boldsymbol{v}_{1ie}(t)$ are bounded for all $t \geq t_0 \geq 0$ and $i \in \mathbb{N}$, from the expression of $\boldsymbol{\Omega}_i$ using properties of the pairwise collision avoidance function β_{ij} in (28) and the smooth step function $h(\chi_{ij}, a_{ij}, b_{ij})$ in (16) with a note that the constants a_{ij} and b_{ij} are chosen as in (32), the limit $\lim_{t\to\infty}\boldsymbol{\Omega}_i(t) = 0$ implies that

$$\begin{cases} \lim_{t\to\infty}(\boldsymbol{\eta}_{1i}(t) - \boldsymbol{\eta}_{1id}(t)) = \mathbf{0}, \\ \lim_{t\to\infty}(\boldsymbol{v}_{1i}(t) - \dot{\boldsymbol{\eta}}_{1id}(t)) = \mathbf{0} \end{cases} \text{or} \begin{cases} \lim_{t\to\infty}(\boldsymbol{\eta}_{1i}(t) - \boldsymbol{\eta}_{1ic}(t)) = \mathbf{0}, \\ \lim_{t\to\infty}(\boldsymbol{v}_{i}(t) - \dot{\boldsymbol{\eta}}_{1ic}(t)) = \mathbf{0}, \end{cases} \tag{83}$$

for all $i \in \mathbb{N}$, i.e., the equilibrium sets can be $(\boldsymbol{\eta}_{1d}, \dot{\boldsymbol{\eta}}_{1d})$ or $(\boldsymbol{\eta}_{1c}, \dot{\boldsymbol{\eta}}_{1c})$ where

$$\begin{aligned} \boldsymbol{\eta}_{1d} &= [\boldsymbol{\eta}_{11d}^T, \cdots, \boldsymbol{\eta}_{1id}^T, \cdots, \boldsymbol{\eta}_{1Nd}^T]^T, \quad \dot{\boldsymbol{\eta}}_{1d} = [\dot{\boldsymbol{\eta}}_{11d}^T, \cdots, \dot{\boldsymbol{\eta}}_{1id}^T, \cdots, \dot{\boldsymbol{\eta}}_{1Nd}^T]^T, \\ \boldsymbol{\eta}_{1c} &= [\boldsymbol{\eta}_{11c}^T, \cdots, \boldsymbol{\eta}_{1ic}^T, \cdots, \boldsymbol{\eta}_{1Nc}^T]^T, \quad \dot{\boldsymbol{\eta}}_{1c} = [\dot{\boldsymbol{\eta}}_{11c}^T, \cdots, \dot{\boldsymbol{\eta}}_{1ic}^T, \cdots, \dot{\boldsymbol{\eta}}_{1Nc}^T]^T. \end{aligned} \tag{84}$$

The vectors $\boldsymbol{\eta}_{1c}$ and $\dot{\boldsymbol{\eta}}_{1c}$ are such that

$$\boldsymbol{\Omega}_{ic} = \boldsymbol{\Omega}_i\big|_{\boldsymbol{\eta}_{1i}=\boldsymbol{\eta}_{1ic}, \boldsymbol{v}_{1i}=\dot{\boldsymbol{\eta}}_{1ic}=\mathbf{0}}, \ \forall i \in \mathbb{N}. \tag{85}$$

The limits (83) mean that $(\boldsymbol{\eta}_1, \boldsymbol{v}_1)$ with $\boldsymbol{\eta}_1 = [\boldsymbol{\eta}_{11}^T, \cdots, \boldsymbol{\eta}_{1i}^T, \cdots, \boldsymbol{\eta}_{1N}^T]^T$ and $\boldsymbol{v}_1 = [\boldsymbol{v}_{11}^T, \cdots, \boldsymbol{v}_{1i}^T, \cdots, \boldsymbol{v}_{1N}^T]^T$ tends to the desired set of equilibrium points $(\boldsymbol{\eta}_{1d}, \dot{\boldsymbol{\eta}}_{1d})$ denoted by $\boldsymbol{E}_d$ or the undesired set of equilibrium points $(\boldsymbol{\eta}_{1c}, \dot{\boldsymbol{\eta}}_{1c})$ denoted by $\boldsymbol{E}_c$. Since it has been shown that the trajectories $(\boldsymbol{\eta}_1, \boldsymbol{v}_1)$ can approach either the desired set $\boldsymbol{E}_d$ or the undesired set $\boldsymbol{E}_c$ 'almost globally'. The term 'almost globally' refers to the fact that the agents start from a set that includes the condition (6) and that does not coincide at any point with the undesired set $\boldsymbol{E}_c$. Hence, we need to prove that $\boldsymbol{E}_d$ is locally asymptotically stable and that $\boldsymbol{E}_c$ is locally unstable. Moreover, we have already proved that the closed-loop system (66) is forward complete and that $\lim_{t\to\infty}\boldsymbol{q}_{ie}(t) = 0$, it therefore is sufficient to consider the first two equations of the closed-loop system (66) to investigate local stability of the sets $\boldsymbol{E}_c$ and $\boldsymbol{E}_d$. In addition, we consider $\boldsymbol{q}_{ie}(t)$ in the term $\frac{\sqrt{\boldsymbol{\Phi}_i^T\boldsymbol{\Phi}_i}}{m_i}\boldsymbol{H}(\boldsymbol{q}_{ie}, \boldsymbol{\alpha}_{\boldsymbol{q}_i})\boldsymbol{e}_3$ in the right hand side of the second equation of the closed-loop system (66) as an input instead of a state.

C. Proof of $\boldsymbol{E}_d$ being asymptotically stable

Linearizing the first two equations of the closed-loop system (66) at $\boldsymbol{\eta}_1 = \boldsymbol{\eta}_{1d}$ and $\boldsymbol{\eta}_1 = \dot{\boldsymbol{\eta}}_{1d}$, gives

$$\begin{aligned} \dot{\boldsymbol{\eta}}_{1e} &= \boldsymbol{v}_{1e}, \\ \dot{\boldsymbol{v}}_{1e} &= -2\boldsymbol{K}\boldsymbol{v}_{1e} - \boldsymbol{C}_1(2\boldsymbol{K}\boldsymbol{\eta}_{1e} + \boldsymbol{v}_{1e}) + \Xi_d, \end{aligned} \tag{86}$$

where $\boldsymbol{\eta}_{1e} = \boldsymbol{\eta}_1 - \boldsymbol{\eta}_{1d}$, $\boldsymbol{v}_{1e} = \boldsymbol{v}_1 - \dot{\boldsymbol{\eta}}_{1d}$, and we have used properties of the pairwise collision avoidance function β_{ij} in (28) and the smooth step function $h(\chi_{ij}, a_{ij}, b_{ij})$ in (16) with a note that the constants a_{ij} and b_{ij} are chosen as in (32). The vector Ξ_d is such that $\lim_{t\to\infty}\boldsymbol{q}_e(t) = 0$ implies that $\lim_{t\to\infty}\Xi_d(t) = 0$ due to the matrix $\boldsymbol{H}(\boldsymbol{q}_{ie}, \boldsymbol{\alpha}_{\boldsymbol{q}_i})$ is defined in (21). It can be seen that the linearized closed-loop system (86) is exponentially stable at the origin since the matrices $\boldsymbol{K}$ and $\boldsymbol{C}_1$ are positive definite, and $\lim_{t\to\infty}\Xi_d(t)=0$.

D. Proof of $\boldsymbol{E}_c$ being unstable

Linearizing the first two equations of the closed-loop system (66) around $\boldsymbol{\eta}_1=\boldsymbol{\eta}_{1c}$ and $\boldsymbol{v}_1=\dot{\boldsymbol{\eta}}_{1c}$ results in

$$\begin{bmatrix}\dot{\boldsymbol{\eta}}_{1i}\\ \dot{\boldsymbol{v}}_{1i}\end{bmatrix}=\frac{\partial \boldsymbol{F}_{1i}}{\partial[\boldsymbol{\eta}_{1i},\ \boldsymbol{v}_{1i}]^T}\Big|_{\boldsymbol{\eta}_{1i}=\boldsymbol{\eta}_{1ic},\boldsymbol{v}_{1i}=\boldsymbol{v}_{1ic}}\begin{bmatrix}\boldsymbol{\eta}_{1i}\\ \boldsymbol{v}_{1i}\end{bmatrix}-\begin{bmatrix}\dot{\eta}_{1id}\\ \ddot{\eta}_{1id}\end{bmatrix}+\Xi_c, \tag{87}$$

where

$$\boldsymbol{F}_{1i}=\begin{bmatrix}\boldsymbol{v}_{1i}\\ (\boldsymbol{\Delta}_i+\boldsymbol{v}_{1ie}\star\boldsymbol{v}_{1ie})^{-1}(-2\boldsymbol{K}\boldsymbol{v}_{1ie}-\boldsymbol{C}_1\boldsymbol{\sigma}(\boldsymbol{\Omega}_i))\end{bmatrix}, \tag{88}$$

and the vector Ξ_c is such that $\lim_{t\to\infty}\boldsymbol{q}_e(t)=0$ implies that $\lim_{t\to\infty}\Xi_c(t)=0$ due to the matrix $\boldsymbol{H}(\boldsymbol{q}_{ie},\boldsymbol{\alpha}_{\boldsymbol{q}_i})$ is defined in (21). We now investigate stability of (87) at $(\boldsymbol{\eta}_{1ic},\dot{\boldsymbol{\eta}}_{1ic})$.

Let $\mathbb{N}^*$ be the set of the aircraft such that if the aircraft i and j belong to the set $\mathbb{N}^*$ then $\chi_{ij}<b_{ij}$ where it is recalled that χ_{ij} is defined in (26) and b_{ij} is chosen as in (32). Also let N^* be the size of the set $\mathbb{N}^*$. For those aircraft in the set $\mathbb{N}^*$, the collision avoidance is active. Let $\boldsymbol{\eta}_{1ijc}=\boldsymbol{\eta}_{1ic}-\boldsymbol{\eta}_{1jc}$, $\boldsymbol{v}_{1ijc}=\boldsymbol{v}_{1ic}-\boldsymbol{v}_{1jc}$ with $\boldsymbol{v}_{1ic}=\dot{\boldsymbol{\eta}}_{1ic}$ and $\boldsymbol{v}_{1jc}=\dot{\boldsymbol{\eta}}_{1jc}$, $\beta'_{ijc}=\beta'_{ij}|_{\boldsymbol{\eta}_{1ij}=\boldsymbol{\eta}_{1ijc},\boldsymbol{v}_{1i}=\dot{\boldsymbol{v}}_{1ic},\boldsymbol{v}_{1j}=\dot{\boldsymbol{v}}_{1jc}}$. Now, from (85) we have

$$\sum_{(i,j)\in\mathbb{N}^*}(2\boldsymbol{K}\boldsymbol{\eta}_{1ijc}+(\boldsymbol{\Delta}_{ic}\boldsymbol{v}_{1ic}-\boldsymbol{\Delta}_{jc}\boldsymbol{v}_{1jc}))^T\boldsymbol{\Omega}_{ijc}=0,\ i\neq j, \tag{89}$$

where $\boldsymbol{\Omega}_{ijc}=\boldsymbol{\Omega}_{ic}-\boldsymbol{\Omega}_{jc}$. Expanding (89) with the use of (85) yields:

$$\begin{aligned}&\sum_{(i,j)\in\mathbb{N}^*}\big(1+N^*\beta'_{ijc}\big)\|2\boldsymbol{K}\boldsymbol{\eta}_{1ijc}+(\boldsymbol{\Delta}_{ic}\boldsymbol{v}_{1ic}-\boldsymbol{\Delta}_{jc}\boldsymbol{v}_{1jc})\|^2=\\ &\qquad\sum_{(i,j)\in\mathbb{N}^*}(2\boldsymbol{K}\boldsymbol{\eta}_{1ijc}+(\boldsymbol{\Delta}_{ic}\boldsymbol{v}_{1ic}-\boldsymbol{\Delta}_{jc}\boldsymbol{v}_{1jc}))^T(2\boldsymbol{K}\boldsymbol{\eta}_{1ijd}+(\boldsymbol{\Delta}_{ic}\dot{\boldsymbol{\eta}}_{1id}-\boldsymbol{\Delta}_{jc}\dot{\boldsymbol{\eta}}_{1jd})),\end{aligned} \tag{90}$$

where $\boldsymbol{\eta}_{1ijd}=\boldsymbol{\eta}_{1id}-\boldsymbol{\eta}_{1jd}$. The sum $\sum_{(i,j)\in\mathbb{N}^*}(2\boldsymbol{K}\boldsymbol{\eta}_{1ijc}+(\boldsymbol{\Delta}_{ic}\boldsymbol{v}_{1ic}-\boldsymbol{\Delta}_{jc}\boldsymbol{v}_{1jc}))^T(2\boldsymbol{K}\boldsymbol{\eta}_{1ijd}+(\boldsymbol{\Delta}_{ic}\dot{\boldsymbol{\eta}}_{1id}-\boldsymbol{\Delta}_{jc}\dot{\boldsymbol{\eta}}_{1jd}))$ is strictly negative since at the point denoted by F where $\boldsymbol{\eta}_{1ij}=\boldsymbol{\eta}_{1ijd}$ and $\boldsymbol{v}_{1i}=\dot{\boldsymbol{\eta}}_{1id}$, $\boldsymbol{v}_{1j}=\dot{\boldsymbol{\eta}}_{1jd}$, $\forall(i,j)\in\mathbb{N}^*,i\neq j$ all attractive and repulsive forces are equal to zero while at the point denoted by C where $\boldsymbol{\eta}_{1ij}=\boldsymbol{\eta}_{1ijc}$, $\boldsymbol{v}_{1ic}=\dot{\boldsymbol{\eta}}_{1ic}$, and $\boldsymbol{v}_{1jc}=\dot{\boldsymbol{\eta}}_{1jc}$, $\forall(i,j)\in\mathbb{N}^*,i\neq j$ the sum of attractive and repulsive forces are equal to zero (but attractive and repulsive forces are nonzero). Therefore the point where $\boldsymbol{\eta}_{1ij}=\boldsymbol{0}$, $\boldsymbol{v}_i=\boldsymbol{0}$ and $\boldsymbol{v}_j=\boldsymbol{0}$, $\forall(i,j)\in\mathbb{N}^*,i\neq j$ must locate between the points F and C for all $(i,j)\in\mathbb{N}^*,i\neq j$, i.e., there exists a strictly positive constant b such that $\sum_{(i,j)\in\mathbb{N}^*}(2\boldsymbol{K}\boldsymbol{\eta}_{1ijc}+(\boldsymbol{\Delta}_{ic}\boldsymbol{v}_{1ic}-\boldsymbol{\Delta}_{jc}\boldsymbol{v}_{1jc}))^T(2\boldsymbol{K}\boldsymbol{\eta}_{1ijd}+(\boldsymbol{\Delta}_{ic}\dot{\boldsymbol{\eta}}_{1id}-\boldsymbol{\Delta}_{jc}\dot{\boldsymbol{\eta}}_{1jd}))\le -b$, which is inserted in (90) to yield

$$\sum_{(i,j)\in\mathbb{N}^*}\big(1+N^*\beta'_{ijc}\big)\|2\boldsymbol{K}\boldsymbol{\eta}_{1ijc}+(\boldsymbol{\Delta}_{ic}\boldsymbol{v}_{1ic}-\boldsymbol{\Delta}_{jc}\boldsymbol{v}_{1jc})\|^2\le -b. \tag{91}$$

This inequality implies that there exists a nonempty set $\mathbb{N}^{**}\subset\mathbb{N}^*$ such that for all $(i,j)\in\mathbb{N}^{**},i\neq j$, $(1+N^{**}\beta'_{ijc})$, where N^{**} is the size of the set $\mathbb{N}^{**}$, is strictly negative, i.e., there exists a strictly negative constant b^{**} such that $(1+N^{**}\beta'_{ijc})\le -b^{**}$ for all $(i,j)\in\mathbb{N}^{**},i\neq j$.

To investigate stability of (87) at $(\boldsymbol{\eta}_{1ic},\dot{\boldsymbol{\eta}}_{1ic})$, we consider the following function for the aircraft belonging to the set $\mathbb{N}^{**}$:

$$V_c=\sum_{(i,j)\in\mathbb{N}^{**},j\neq i}\sqrt{\|\boldsymbol{K}(\boldsymbol{\eta}_{1ij}-\boldsymbol{\eta}_{1ijc})+\boldsymbol{\Delta}_{Lc}(\boldsymbol{v}_{1ij}-\boldsymbol{v}_{1ijc})\|^2+1}, \tag{92}$$

where $\boldsymbol{\Delta}_{Lc}=\frac{\partial\boldsymbol{\Delta}_i}{\partial\boldsymbol{v}_{1i}}\big|_{\boldsymbol{v}_{1i}=\boldsymbol{v}_{ic}}$ and it is noted that $\frac{\partial\boldsymbol{\Delta}_i}{\partial\boldsymbol{v}_{1i}}\big|_{\boldsymbol{v}_{1i}=\boldsymbol{v}_{ic}}=\frac{\partial\boldsymbol{\Delta}_j}{\partial\boldsymbol{v}_{1i}}\big|_{\boldsymbol{v}_{1j}=\boldsymbol{v}_{jc}}$ since $\dot{\boldsymbol{\eta}}_{1ic}=\dot{\boldsymbol{\eta}}_{1jc}=\boldsymbol{0}$. Differentiating both sides of (92) along the solutions of (87) in the subspace defined by $\boldsymbol{K}(\boldsymbol{\eta}_{1ij}-\boldsymbol{\eta}_{1ijc})+\boldsymbol{\Delta}_{Lc}(\boldsymbol{v}_{1ij}-\boldsymbol{v}_{1ijc})=\boldsymbol{0}$ for all $(i,j)\in\mathbb{N}\setminus\mathbb{N}^{**}$ and $(\boldsymbol{K}\boldsymbol{\eta}_{1ijc}+\boldsymbol{\Delta}_{Lc}\boldsymbol{v}_{1ijc})^T(\boldsymbol{K}(\boldsymbol{\eta}_{1ij}-\boldsymbol{\eta}_{1ijc})+\boldsymbol{\Delta}_{Lc}(\boldsymbol{v}_{1ij}-\boldsymbol{v}_{1ijc}))=0$ for all $(i,j)\in\mathbb{N}^*,i\neq j$ satisfies

$$\begin{aligned}\dot V_c\ge\ & b^{**}\sum_{(i,j)\in\mathbb{N}^{**}}\frac{(\boldsymbol{K}(\boldsymbol{\eta}_{1ij}-\boldsymbol{\eta}_{1ijc})+\boldsymbol{\Delta}_{Lc}(\boldsymbol{v}_{1ij}-\boldsymbol{v}_{1ijc}))^T\boldsymbol{C}(\boldsymbol{K}(\boldsymbol{\eta}_{1ij}-\boldsymbol{\eta}_{1ijc})+\boldsymbol{\Delta}_{Lc}(\boldsymbol{v}_{1ij}-\boldsymbol{v}_{1ijc}))}{\sqrt{\|\boldsymbol{K}(\boldsymbol{\eta}_{1ij}-\boldsymbol{\eta}_{1ijc})+\boldsymbol{\Delta}_{Lc}(\boldsymbol{v}_{1ij}-\boldsymbol{v}_{1ijc})\|^2+1}}+\\ &\sum_{(i,j)\in\mathbb{N}^{**}}\frac{(\boldsymbol{K}(\boldsymbol{\eta}_{1ij}-\boldsymbol{\eta}_{1ijc})+\boldsymbol{\Delta}_{Lc}(\boldsymbol{v}_{1ij}-\boldsymbol{v}_{1ijc}))^T\Xi_c}{\sqrt{\|\boldsymbol{K}(\boldsymbol{\eta}_{1ij}-\boldsymbol{\eta}_{1ijc})+\boldsymbol{\Delta}_{Lc}(\boldsymbol{v}_{1ij}-\boldsymbol{v}_{1ijc})\|^2+1}},\end{aligned} \tag{93}$$

where we have used $(1 + N^{**}\beta'_{ijc}) \leq -b^{**}$ for all $(i, j) \in \mathbb{N}^{**}, i \neq j$. Local instability of $(\boldsymbol{\eta}_{1ijc}, \boldsymbol{v}_{1ijc})$ for all $(i, j) \in \mathbb{N}^{**}, i \neq j$ directly follows from (92) and (93) with a note that b^{**} is a strictly positive constant and that $\lim_{t\to\infty} \boldsymbol{\Xi}_c(t) = 0$. This in turn implies that the set $\boldsymbol{E}_c$ is unstable. □

REFERENCES

[1] K. D. Do and J. Pan, *Control of Ships and Underwater Vehicles: Design for Underactuated and Nonlinear Marine Systems*. Springer, 2009.

[2] J. Hauser, S. Sastry, and G. Meyer, "Nonlinear control design for slightly non-minimum phase systems: application to V/STOL aircraft," *Automatica*, vol. 28, no. 4, pp. 665–679, 1992.

[3] C.-S. Huang and K. Yuan, "Output tracking of a nonlinear non-minimum phase PVTOL aircraft based on nonlinear state feedback," *International Journal of Control*, vol. 75, no. 6, pp. 466–473, 2002.

[4] F. Lin, W. Zhang, and R. Brandt, "Robust hovering control of a PVTOL aircraft," *IEEE Transactions on Control Systems Technology*, vol. 7, no. 3, pp. 343–351, 1999.

[5] P. Martin, S. Devasia, and B. Paden, "A different look at output tracking control of a VTOL aircraft," *Automatica*, vol. 32, no. 1, pp. 101–107, 1996.

[6] R. Olfati-Saber, "Global configuration stabilization for the VTOL aircraft with strong input coupling," *IEEE Transactions on Automatic Control*, vol. 47, no. 11, pp. 1949–1952, 2002.

[7] K. D. Do, Z. P. Jiang, and J. Pan, "Global tracking control of a VTOL aircraft without velocity measurements," *IEEE Transactions on Automatic Control*, vol. 48, no. 12, pp. 2212–2217, 2003.

[8] P. Setlur, D. Dawson, Y. Fang, and B. Costic, "Nonlinear tracking control of the VTOL aircraft," *Proceedings of the 40th IEEE Conference on Decision and Control, Florida USA*, pp. 4592–4597, 2001.

[9] P. Castillo, A. Dzul, and R. Lozano, "Real-time stabilization and tracking of a four-rotor mini rotorcraft," *IEEE Transactions on Control Systems Technology*, vol. 12, no. 4, pp. 510–516, 2004.

[10] T. Madani and A. Benallegue, "Control of a quadrotor mini-helicopter via full state backstepping technique," *Proceedings of the 45th IEEE Conference on Decision & Control*, pp. 1515–1520, 2006.

[11] Z. Zuo, "Trajectory tracking control design with command-filtered compensation for a quadrotor," *IET Control Theory and Applications*, vol. 4, no. 11, pp. 1515–1520, 2010.

[12] S. M. Joshi, A. G.Kelkar, and J. T.-Y.Wen, "Robust attitude stabilization of spacecraft using nonlinear quaternion feedback," *IEEE Transactions on Automatic Control*, vol. 40, no. 10, pp. 1800–1803, 1995.

[13] A. Tayebi and S. McGilvray, "Attitude stabilization of a VTOL quadrotor aircraft," *IEEE Transactions on Control Systems Technology*, vol. 14, no. 3, pp. 562–571, 2006.

[14] A. Abdessameud and A. Tayebi, "Global trajectory tracking control of VTOL-UAVs without linear velocity measurements," *Automatica*, vol. 46, pp. 1053–1059, 2010.

[15] A. Roberts and A. Tayebi, "Adaptive position tracking of VTOL UAVs," *IEEE Transactions on Robotics*, vol. 27, no. 1, pp. 129–142, 2011.

[16] A. Zavala-Rio, I. Fantoni, and R. Lozano, "Global stabilization of a pvtol aircraft model with bounded inputs," *International Journal of Control*, vol. 76, no. 18, pp. 1833–1844, 2003.

[17] P. Castillo, A. Dzul, and R. Lozano, "Real-time stabilization and tracking of a four-rotor mini rotorcraft," *IEEE Transactions on Control Systems Technology*, vol. 12, no. 4, pp. 510–516, 2004.

[18] A. Ailon, "Simple tracking controllers for autonomous VTOL aircraft with bounded inputs," *IEEE Transactions on Automatic Control*, vol. 55, pp. 737–743, 2010.

[19] A. Zavala-Rio, I. Fantoni, and G. Sanahuja, "Finite-time observer-based output-feedback control for the global stabilisation of the pvtol aircraft with bounded inputs," *International Journal of Systems Science*, pp. 1–20, 2014.

[20] A. R. Teel, "Global stabilization and restricted tracking for multiple integrators with bounded control," *Systems and Control Letters*, vol. 18, no. 3, pp. 165–171, 1992.

[21] P. Wang, "Navigation strategies for multiple autonomous mobile robots moving in formation," *Journal of Robotic Systems*, vol. 8, no. 2, pp. 177–195, 1991.

[22] A. Das, R. Fierro, V. Kumar, J. Ostrowski, J. Spletzer, and C. Taylor, "A vision based formation control framework," *IEEE Transactions on Robotics and Automation*, vol. 18, no. 5, pp. 813–825, 2002.

[23] D. Gu and Z. Wang, "Leader−follower flocking: Algorithms and experiments," *IEEE Transactions on Control Systems Technology*, vol. 17, no. 5, pp. 1211–1219, 2009.

[24] J. Hu and G. Feng, "Distributed tracking control of leader−follower multi-agent systems under noisy measurement," *Automatica*, vol. 46, no. 8, pp. 1382–1387, 2010.

[25] M. Egerstedt and X. Hu, "Formation constrained multiagent control," *IEEE Transactions on Robotics and Austomation*, vol. 17, no. 6, pp. 947–951, 2001.

[26] T. Balch and R. C. Arkin, "Behavior-based formation control for multirobot teams," *IEEE Transactions on Robotics and Automation*, vol. 14, no. 6, pp. 926–939, 1998.

[27] R. T. Jonathan, R. W. Beard, and B. Young, "A decentralized approach to formation maneuvers," *IEEE Transactions on Robotics and Automation*, vol. 19, no. 6, pp. 933–941, 2003.

[28] D. M. Stipanovic, G. Inalhan, R. Teo, and C. J. Tomlin, "Decentralized overlapping control of a formation of unmanned aerial vehicles," *Automatica*, vol. 40, no. 8, pp. 1285–1296, 2004.

[29] K. D. Do, "Bounded controllers for formation stabilization of mobile agents with limited sensing ranges," *IEEE Transactions on Automatic Control*, vol. 52, no. 3, pp. 569–576, 2007.

[30] I. Hussein and A. Bloch, "Optimal control of underactuated nonholonomic mechanical systems," *IEEE Transactions on Automatic Control*, vol. 53, no. 3, pp. 668–681, 2008.

[31] F. Cucker and J. G. Dong, "Avoiding collisions in flocks," *IEEE Transactions on Automatic Control*, vol. 55, no. 5, pp. 1238–1243, 2010.

[32] A. Abdessameuda and A. Tayebi, "On consensus algorithms for double-integrator dynamics without velocity measurements and with input constraints," *Systems and Control Letters*, vol. 59, no. 5, pp. 812–821, 2010.

[33] R. Olfati-Saber, "Flocking for multi-agent dynamic systems: algorithms and theory," *IEEE Transactions on Automatic Control*, vol. 51, no. 3, pp. 401–420, 2006.

[34] D. Dimarogonas and K. Kyriakopoulos, "A feedback control scheme for multiple independent dynamic non-point agents," *International Journal of Control*, vol. 79, no. 12, pp. 1613–1623, 2006.
[35] H. Yang, Z. Zhang, and S. Zhang, "Consensus of second-order multi-agent systems with exogenous disturbances," *International Journal of Robust and Nonlinear Control*, vol. 21, pp. 945–956, 2011.
[36] Y. Hu, H. Su, and J. Lam, "Adaptive consensus with a virtual leader of multiple agents governed by locally lipschitz nonlinearity," *International Journal of Robust and Nonlinear Control, In press*, 2012.
[37] K. D. Do, "Bounded assignment formation control of second-order dynamic agents," *IEEE/ASME Transactions on Mechatronics*, vol. 19, no. 2, pp. 477–489, 2014.
[38] F. Fahimi, "Full formation control for autonomous helicopter groups," *Robotica*, vol. 26, pp. 143–156, 2008.
[39] T. Lee, K. Sreenath, and V. Kumar, "Geometric control of cooperating multiple quadrotor UAVs with a suspended load," *Proceedings of the IEEE Conference on Decision and Control*, pp. 5510–5515, 2013.
[40] V. Roldao, R. Cunha, D. Cabecinhas, C. Silvestre, and P. Oliveira, "A leader-following trajectory generator with application to quadrotor formation flight," *Robotics and Autonomous Systems*, vol. 62, pp. 1597–1609, 2014.
[41] D. A. Mercado, R. Castro, and R. Lozano, "Quadrotors flight formation control using a leader-follower approach," *Proceedings of European Control Conference*, pp. 3858–3863, 2013.
[42] A. Abdessameud and A. Tayebi, "Formation control of VTOL UAVs without linear-velocity measurements," *Proceedings of American Control Conference*, pp. 2107–2112, 2010.
[43] A. Abdessameud and A. Tayebi, "Formation control of VTOL unmanned aerial vehicles with communication delays," *Automatica*, vol. 47, pp. 2382–2394, 2011.
[44] L. Garcia-Delgado, A. Dzul, V. Santibanez, and M. Llama, "Quad-rotors formation based on potential functions with obstacle avoidance," *IET Control Theory and Applications*, vol. 6, no. 12, pp. 1787–1802, 2012.
[45] K. D. Do, "Global tracking control of underactuated ODINs in three-dimensional space," *International Journal of Control*, pp. 1–14, 2012.
[46] S. S. Ge and Y. J. Cui, "New potential functions for mobile robot path planning," *IEEE Transactions on Robotics and Automation*, vol. 16, no. 5, pp. 615–620, 2000.
[47] K. D. Do, "Coordination control of multiple ellipsoidal agents with collision avoidance and limited sensing ranges," *Systems & Control Letters*, vol. 61, no. 1, pp. 247–257, 2012.
[48] P. Ogren, E. Fiorelli, and N. E. Leonard, "Cooperative control of mobile sensor networks: Adaptive gradient climbing in a distributed environment," *IEEE Transactions on Automatic Control*, vol. 49, no. 8, pp. 1292–1302, 2004.
[49] N. Marchand and A. Hably, "Global stabilization of multiple integrators with bounded controls," *Automatica*, vol. 41, no. 12, pp. 2147–2152, 2005.
[50] H. Khalil, *Nonlinear Systems*. Prentice Hall, 2002.
[51] M. Krstic, I. Kanellakopoulos, and P. Kokotovic, *Nonlinear and Adaptive Control Design*. New York: Wiley, 1995.
[52] D. Liberzon, *Switching in Systems and Control*. Birkauser, 2003.